The Abdus Salam
International Centre for Theoretical Physics

United Nations
Educational, Scientific and
Cultural Organization

IAEA
International Atomic Energy Agency

SMR 2333-40

Workshop on Science Applications of GNSS in Developing Countries (11-27 April), followed by the: Seminar on Development and Use of the Ionospheric NeQuick Model (30 April-1 May)

11 April - 1 May, 2012

Iono-Seismic Effects Detection Using GNSS Observations

PULINETS Sergey Alexander
Fyodorov Institute of Applied Geophysics,
Rostokinskaya str. 9
129128 Moscow
Russia
RUSSIAN FEDERATION

Iono-Seismic Effects Detection Using GNSS Observations

Sergey Pulinets

Space Research Institute, RAS, Moscow
Fiodorov Institute of Applied Geophysics

With contribution from Tiger Liu, Liming He, Katsumi Hattori, Maxim Klimenko, Luigi Ciraolo, Viacheslav Kunitsyn, Dimitar Ouzounov, Dmitri Davidenko, Konstantin Tsybulya, Marina Tsidilina, Michel Parrot

ИНСТИТУТ КОСМИЧЕСКИХ ИССЛЕДОВАНИЙ РАН

Space Weather and Ionospheric Exploration with GNSS, ICTP, Trieste, April, 2012

Outline

1. For detection we should know what to detect

* Basic physical processes of seismo-ionospheric effects
* Main phenomenology
* Modeling
* Statistics

2. Examples
3. Detection

* Precursor mask
* Cross-correlation coefficient
* Local variability index
* Regional TEC

4. Synergy of the processes of earthquake preparation
5. Conclusions

Mechanism of formation of cluster ions in the lower troposphere

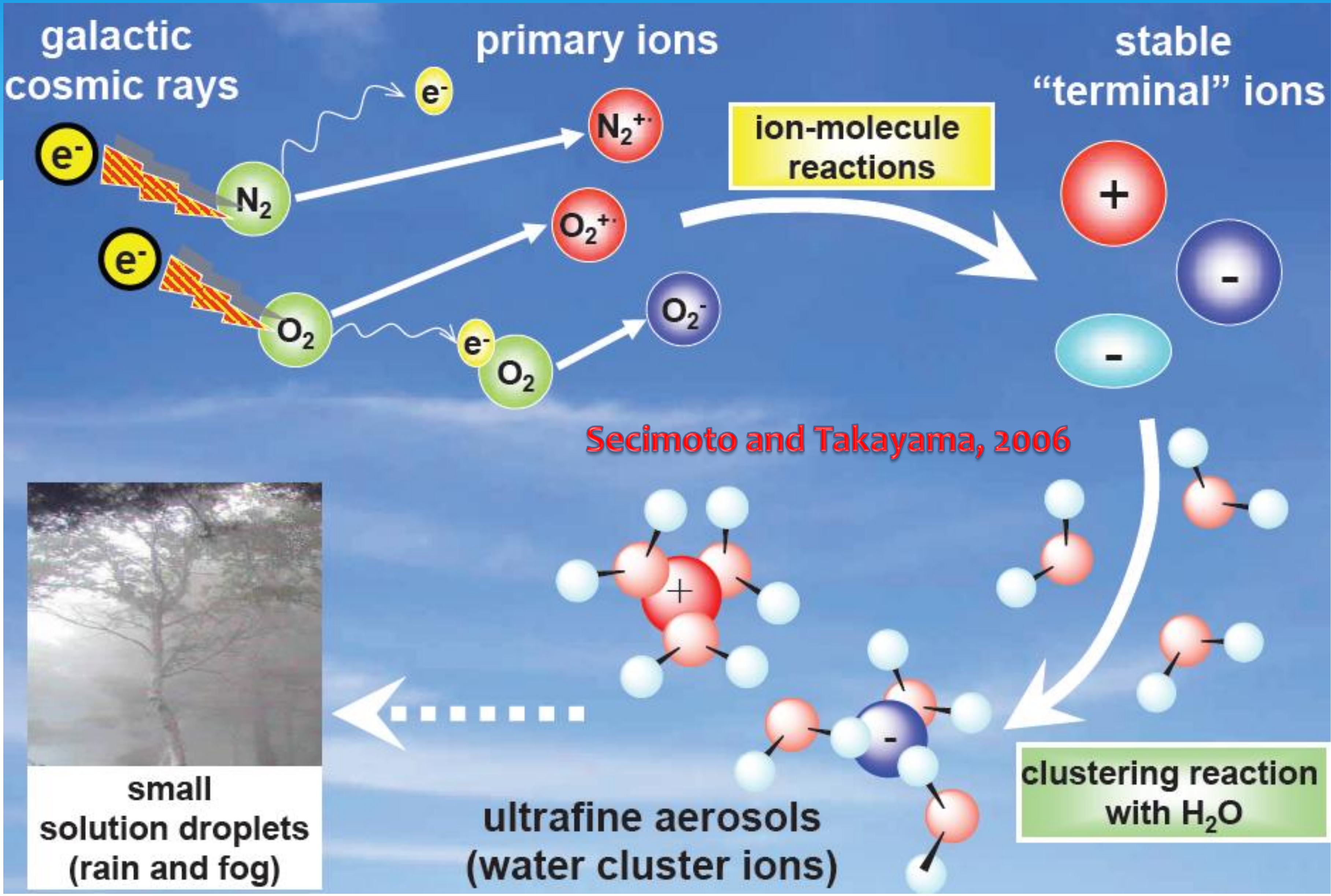

ИКИ
ИНСТИТУТ КОСМИЧЕСКИХ ИССЛЕДОВАНИЙ РАН

Ion-molecular reactions

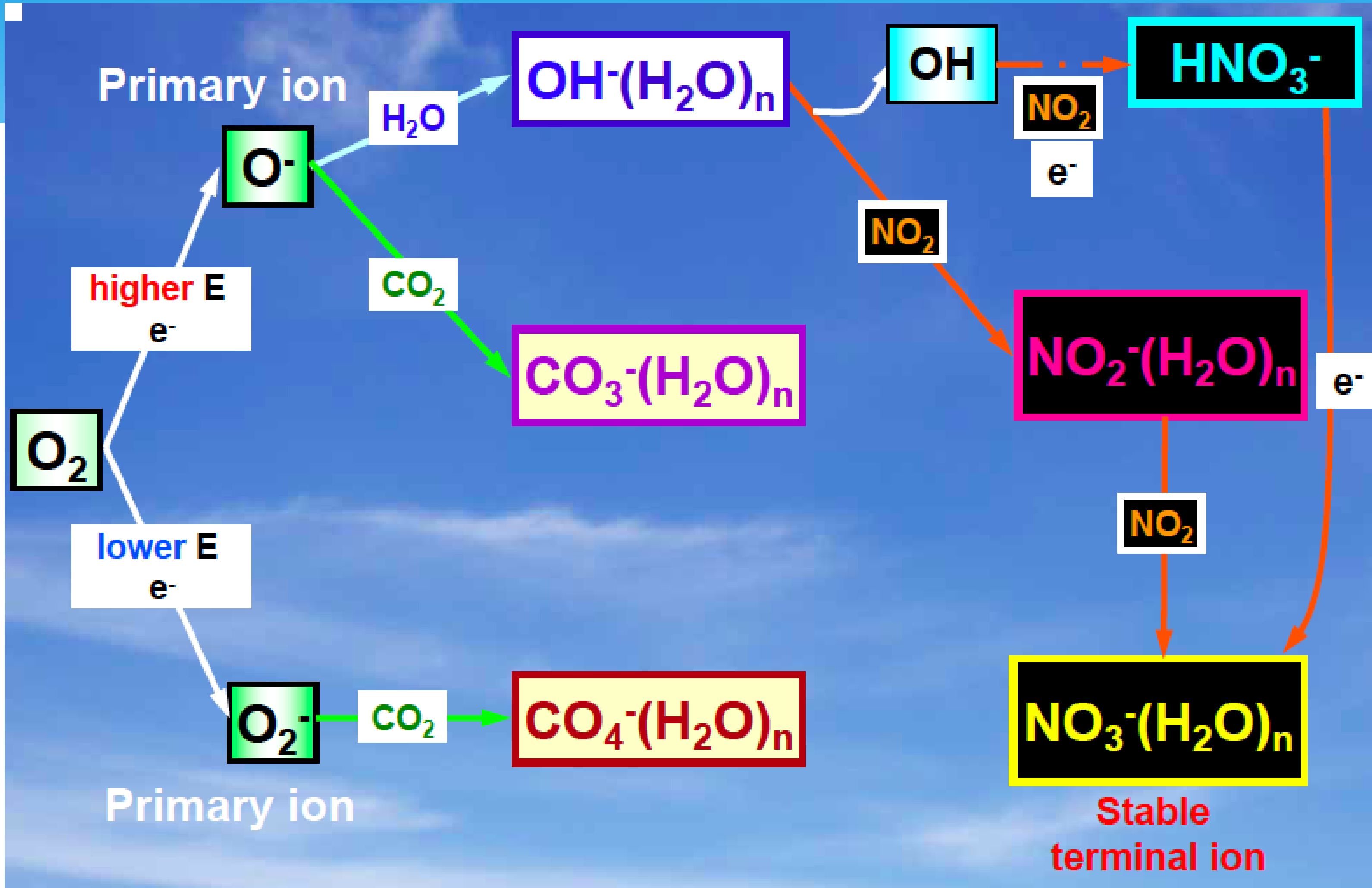

Sequential progress of the ion-molecule reactions for NO_x^- and CO_x^-.

F.C. Fehsenfeld et al. *J. Chem. Phys* 61(1974)p. 3181

ИКИ
ИНСТИТУТ КОСМИЧЕСКИХ ИССЛЕДОВАНИЙ РАН

Hydration process

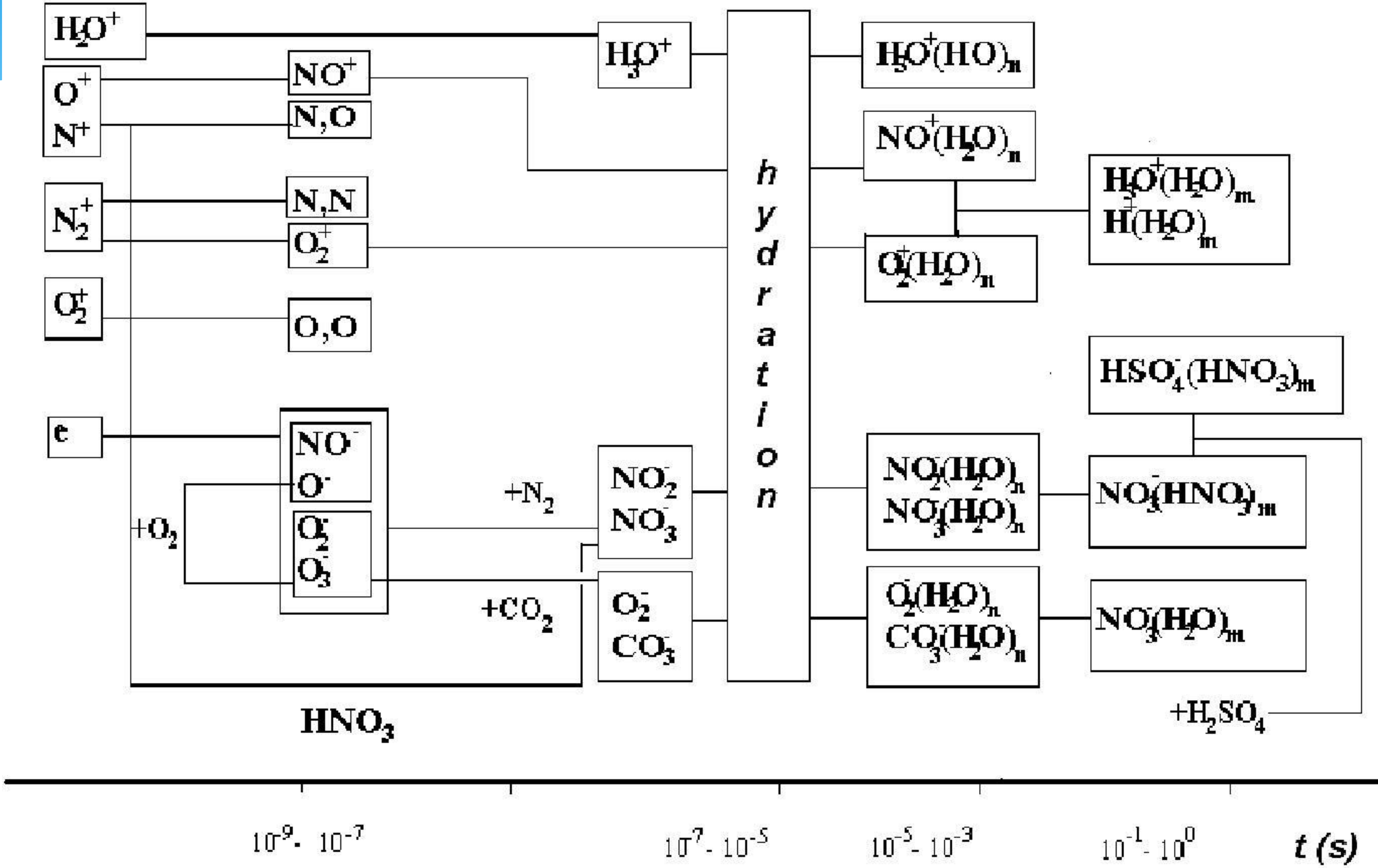

ИНСТИТУТ КОСМИЧЕСКИХ ИССЛЕДОВАНИЙ РАН

Droplets formation

UCN Utrafine nuclei of condensation
CN Condensation Nuclei
CCN Cloud Condensation Nuclei

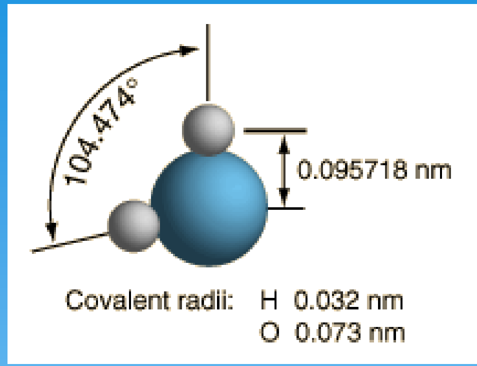

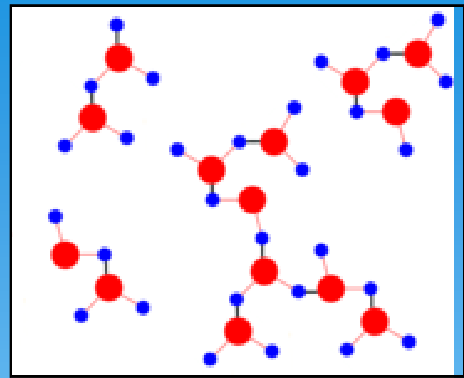

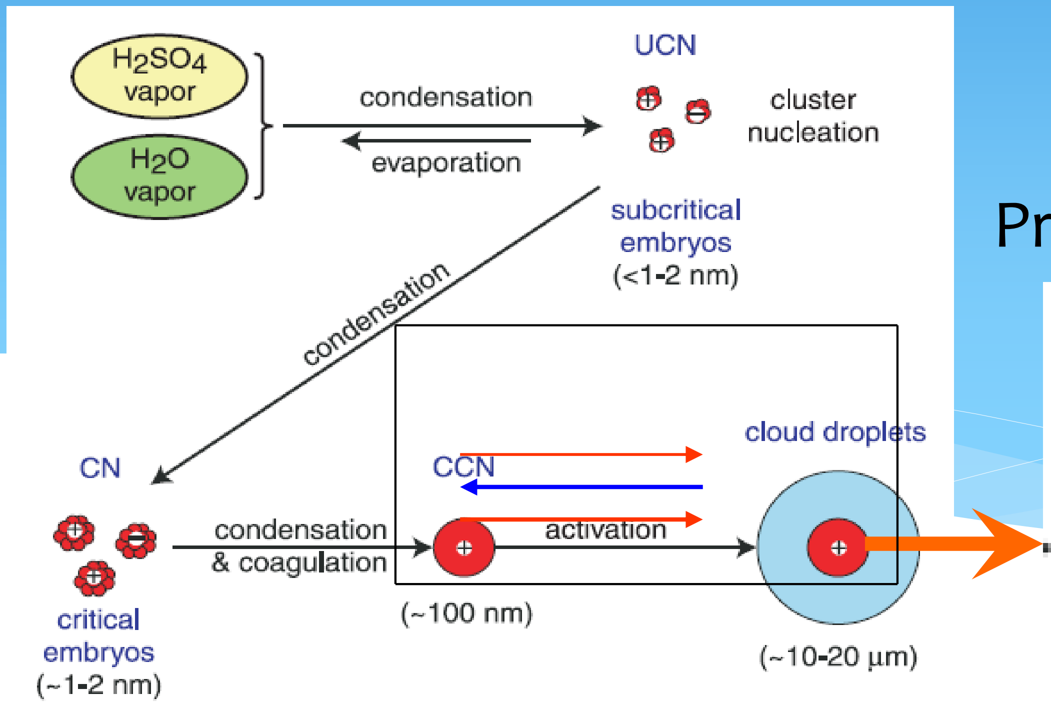

Precipitation droplet

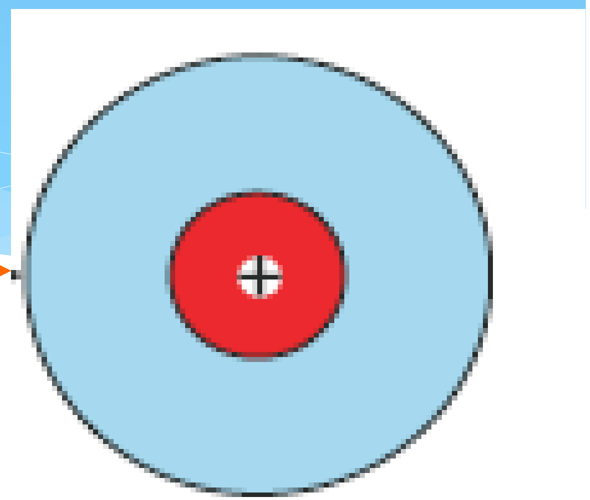

Usually 3 cycles of the droplet formation are realized

Typical radon variations before earthquake

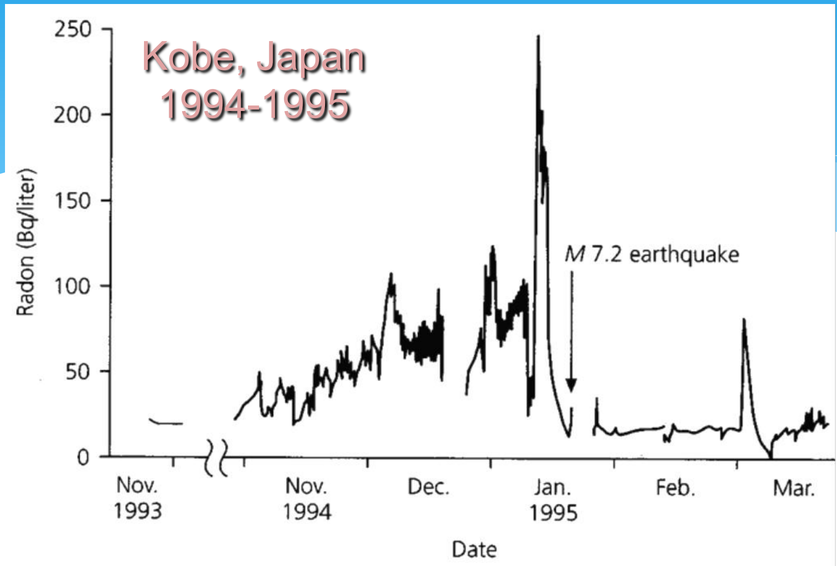

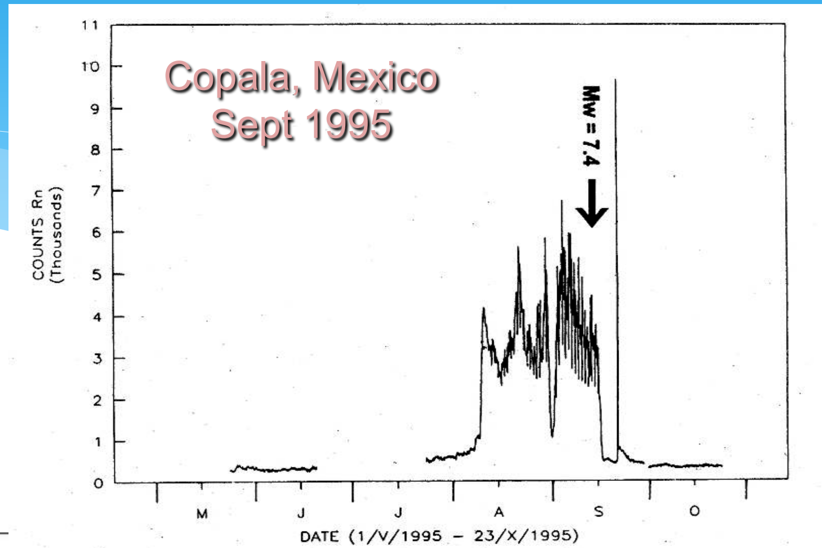

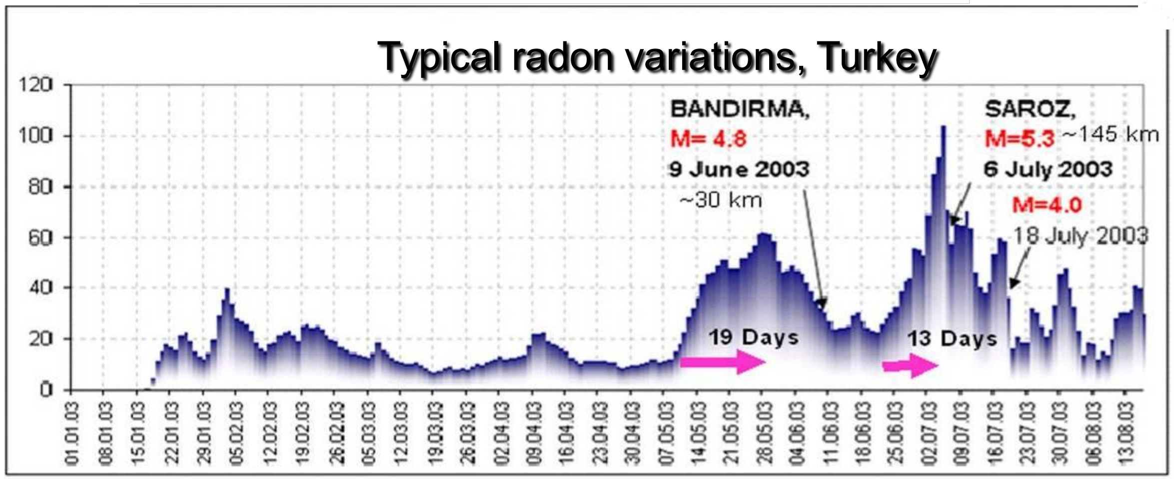

L'Aquila, Italy
April 2009

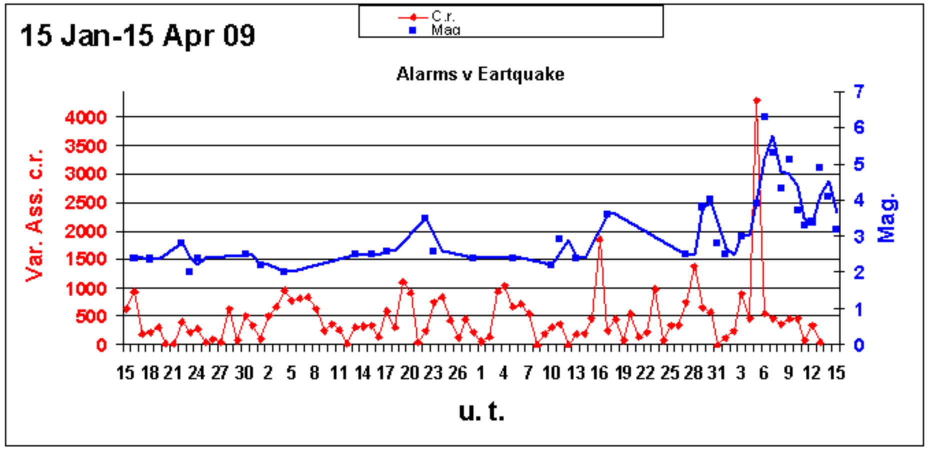

ИНСТИТУТ
КОСМИЧЕСКИХ
ИССЛЕДОВАНИЙ
РАН

Do large aerosol-size clusters form before earthquakes?

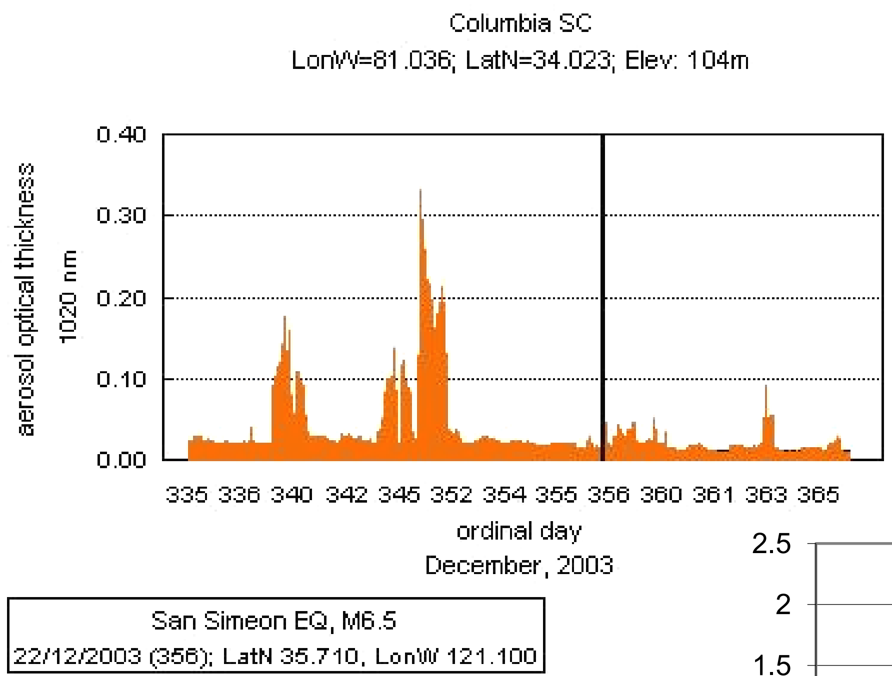

Van earthquake M7.2 in Turkey 23 Oct 2011

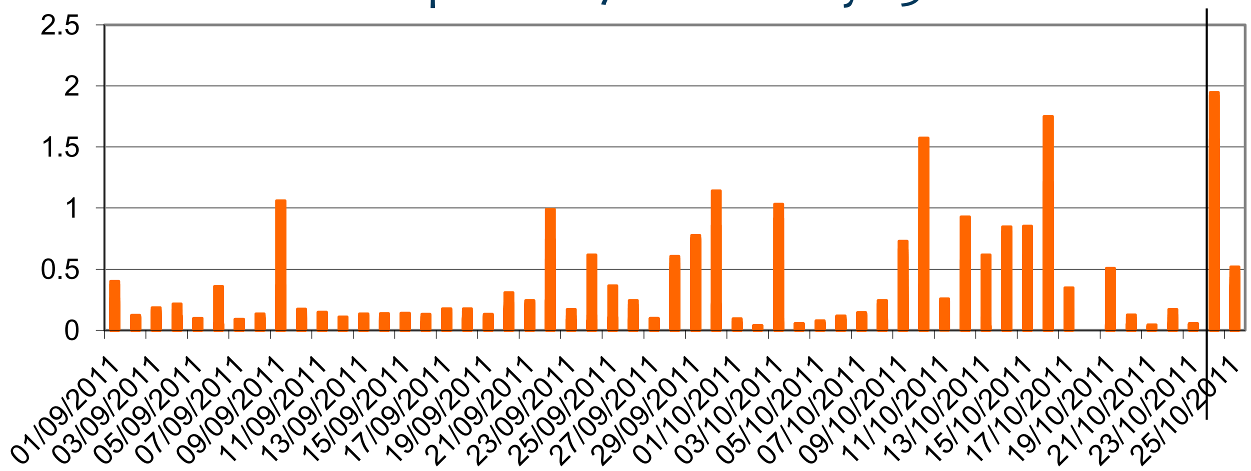

What relation all this has to the ionosphere?

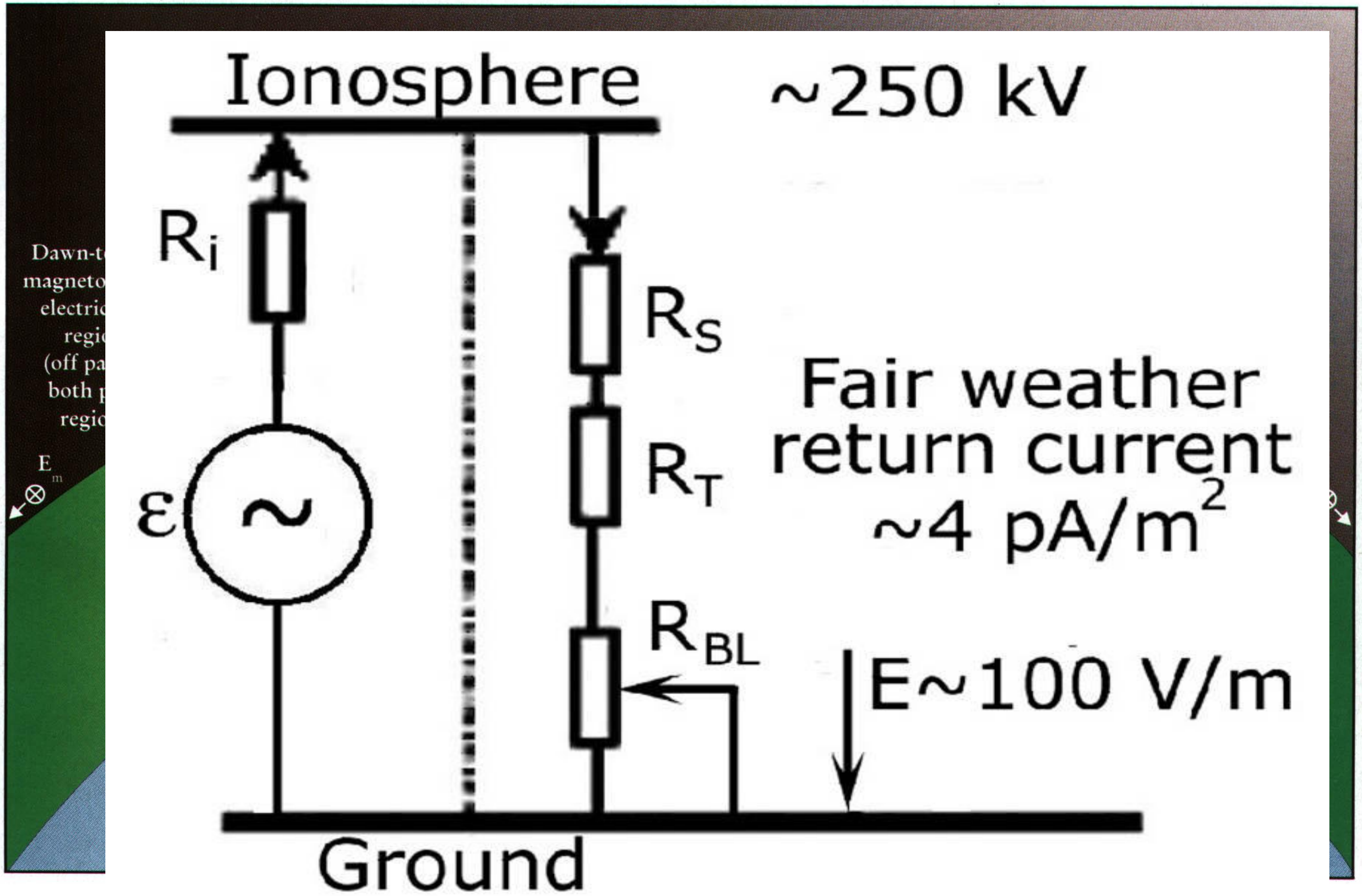

Ion's mobility and air conductivity

$$i = e\left(n^{+}\mu^{+} + n^{-}\mu^{-}\right)E = \sigma E$$

$$\sigma = e\left(n^{+}\mu^{+} + n^{-}\mu^{-}\right)$$

$$\sigma = e\sum_{i=1}^{n}\left(n_i^{+}\mu_i^{+} + n_i^{-}\mu_i^{-}\right)$$

Analyzer	Fraction	Mobility $cm^2 V^{-1} s^{-1}$	Diameter nm
		Small Cluster Ions	
IS_1	N_1/P_1	2.51–3.14	0.36–0.45
IS_1	N_2/P_2	2.01–2.51	0.45–0.56
IS_1	N_3/P_3	1.60–2.01	0.56–0.70
IS_1	N_4/P_4	1.28–1.60	0.70–0.85
		Big Cluster Ions	
IS_1	N_5/P_5	1.02–1.28	0.85–1.03
IS_1	N_6/P_6	0.79–1.02	1.03–1.24
IS_1	N_7/P_7	0.63–0.79	1.24–1.42
IS_1	N_8/P_8	0.50–0.63	1.42–1.60
		Intermediate Ions	
IS_1	N_9/P_9	0.40–0.50	1.6–1.8
IS_1	N_{10}/P_{10}	0.32–0.40	1.8–2.0
IS_1	N_{11}/P_{11}	0.25–0.32	2.0–2.3
IS_2	N_{12}/P_{12}	0.150–0.293	2.1–3.2
IS_2	N_{13}/P_{13}	0.074–0.150	3.2–4.8
IS_2	N_{14}/P_{14}	0.034–0.074	4.8–7.4
		Light Large Ions	
IS_2	N_{15}/P_{15}	0.016–0.034	7.4–11.0
IS_3	N_{16}/P_{16}	0.0091–0.0205	9.7–14.8
IS_3	N_{17}/P_{17}	0.0042–0.0091	15–22
		Heavy Large Ions	
IS_3	N_{18}/P_{18}	0.00192–0.00420	22–34
IS_3	N_{19}/P_{19}	0.00087–0.00192	34–52
IS_3	N_{20}/P_{20}	0.00041–0.00087	52–79

ИКИ
ИНСТИТУТ КОСМИЧЕСКИХ ИССЛЕДОВАНИЙ РАН

Ionospheric potential variations

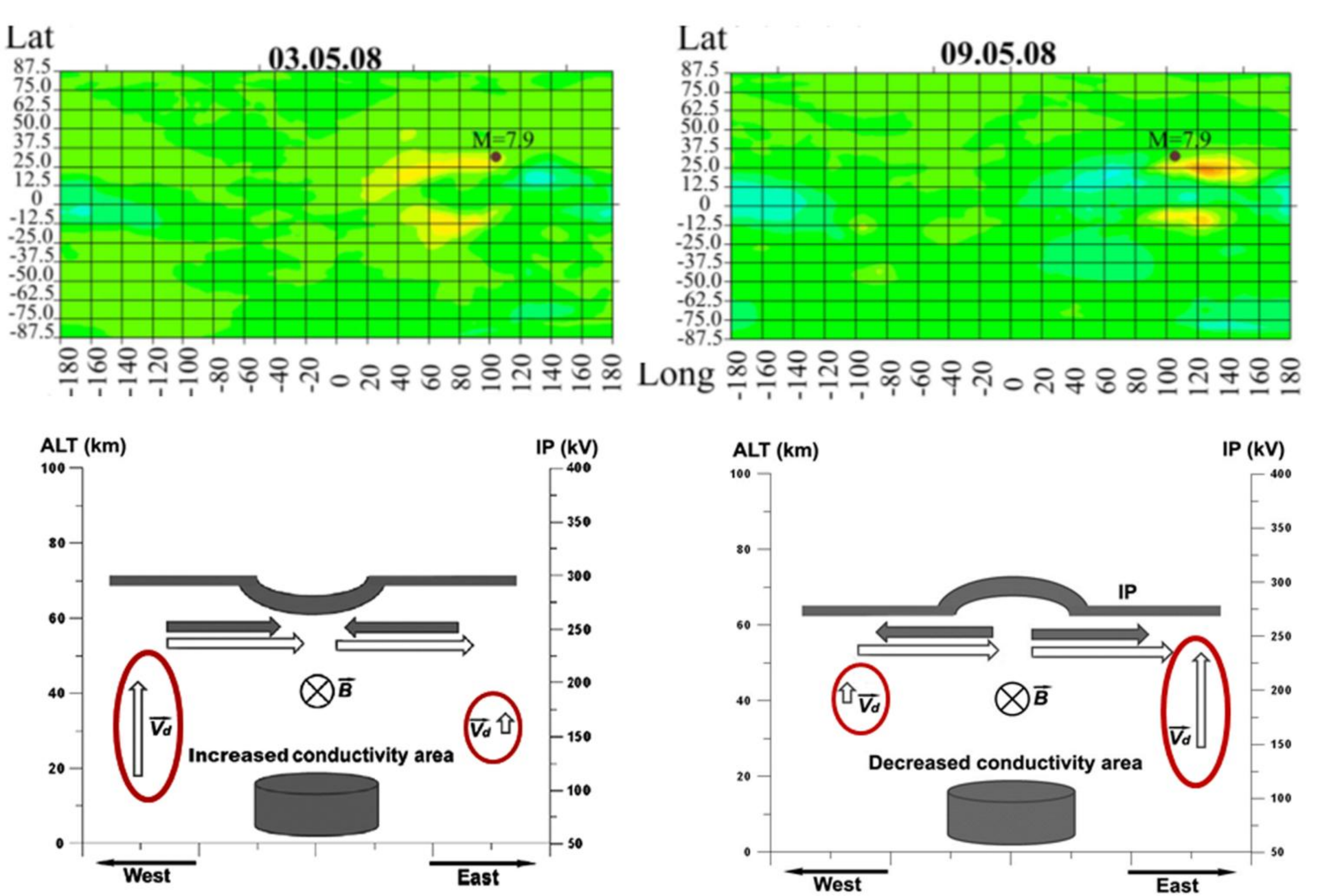

ИНСТИТУТ КОСМИЧЕСКИХ ИССЛЕДОВАНИЙ РАН

Ion concentration distribution before Sumatra M8.7 EQ of 27 March 2005

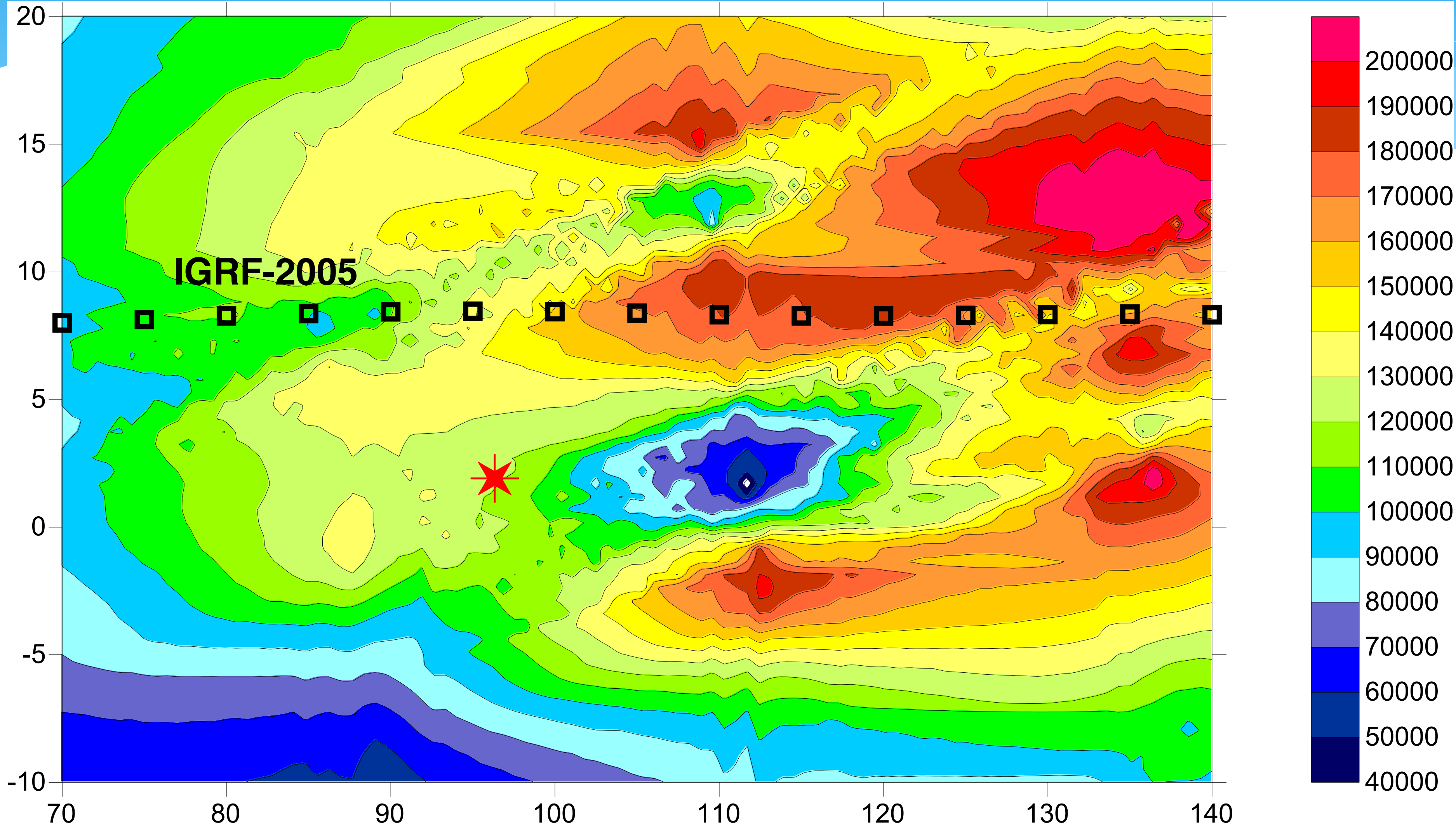

ИКИ
ИНСТИТУТ КОСМИЧЕСКИХ ИССЛЕДОВАНИЙ РАН

Plasma bubbles

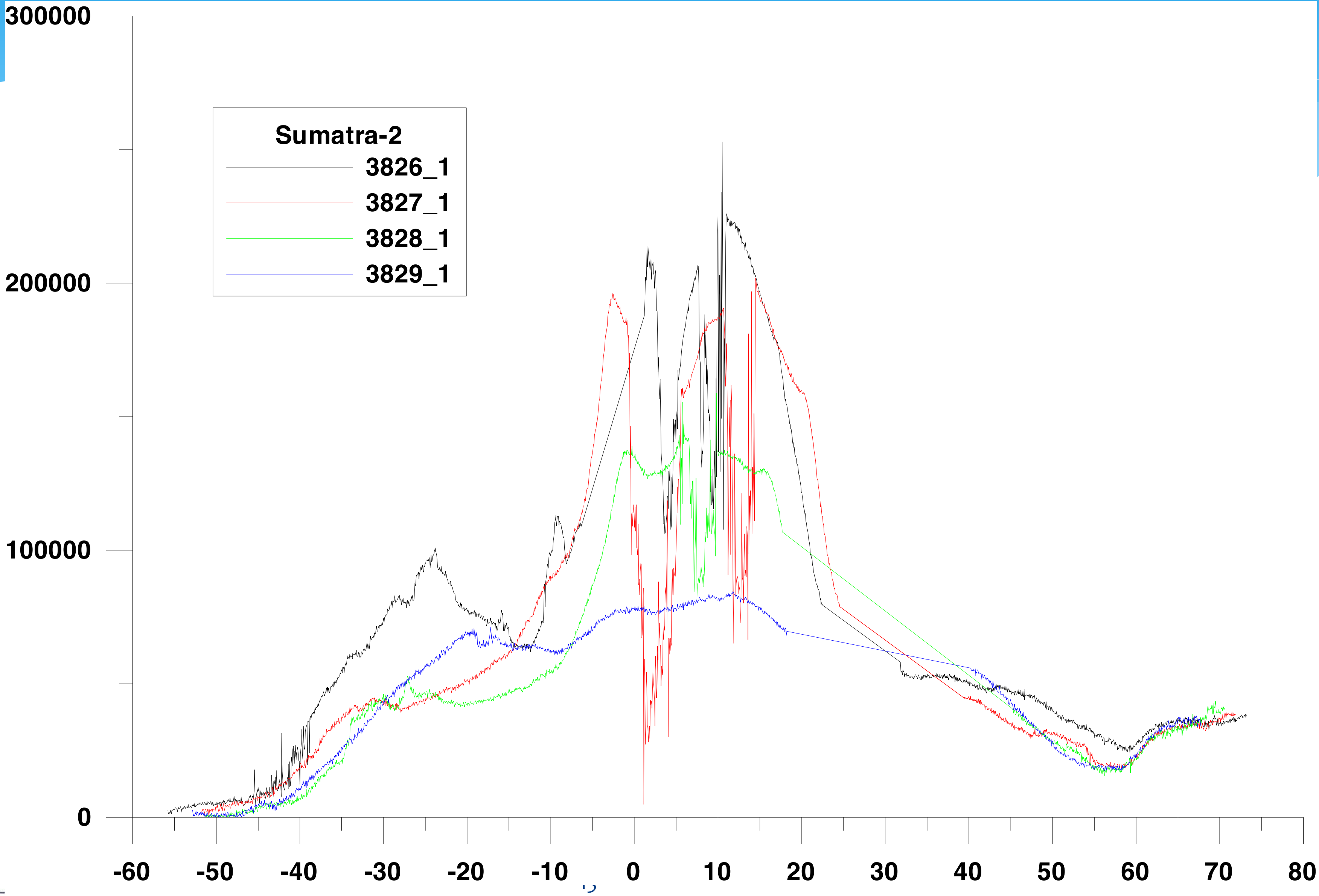

March 22

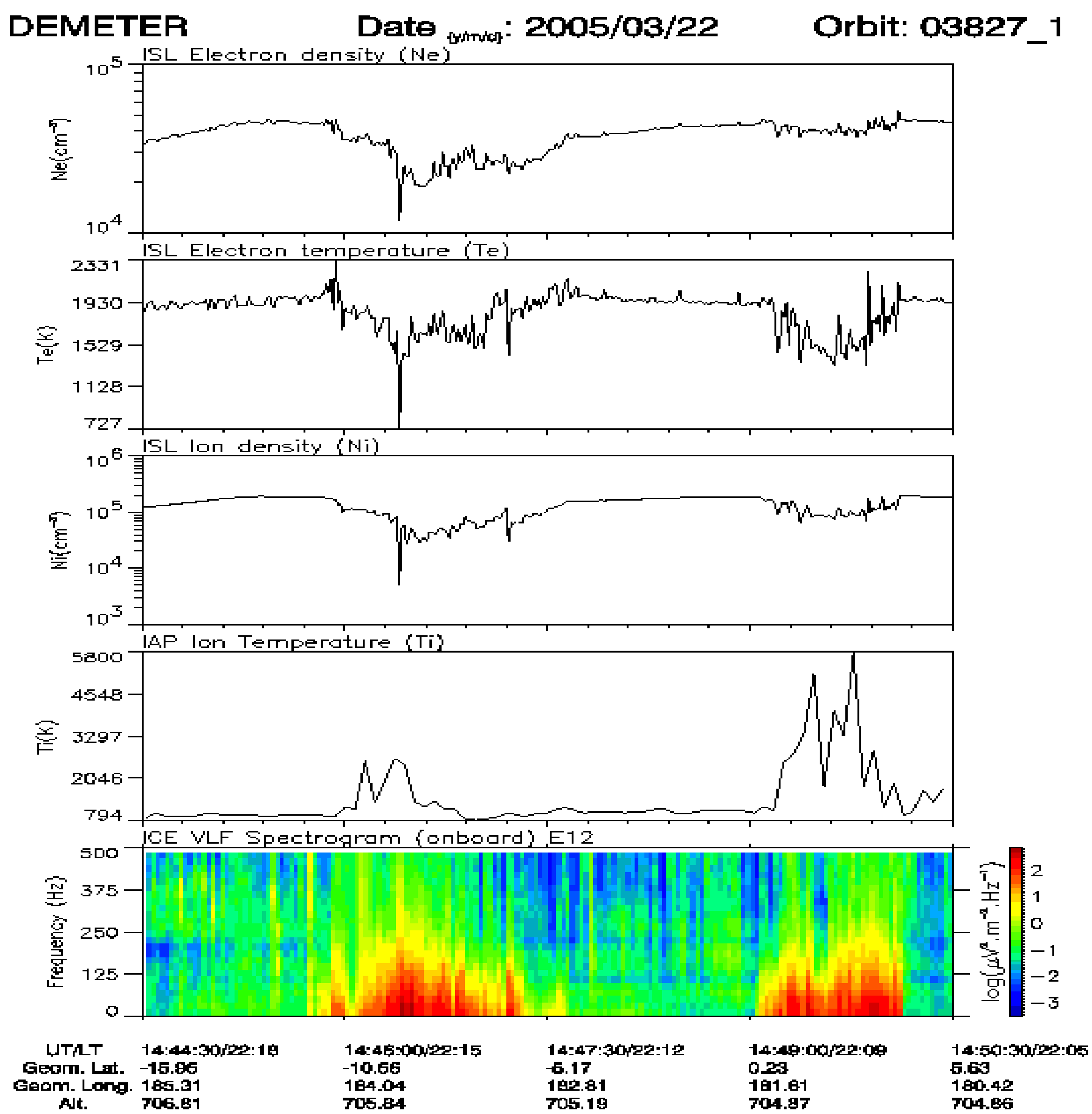
DEMETER
Date (y/m/d): 2005/03/22
Orbit: 03827_1
ISL Electron density (Ne)
Ne(cm⁻³)
ISL Electron temperature (Te)
Te(K)
ISL Ion density (Ni)
Ni(cm⁻³)
IAP Ion Temperature (Ti)
Ti(K)
ICE VLF Spectrogram (onboard) E12
Frequency (Hz)
UT/LT 14:44:30/22:18 14:46:00/22:15 14:47:30/22:12 14:49:00/22:09 14:50:30/22:05
Geom. Lat. -15.86 -10.66 -5.17 0.23 5.63
Geom. Long. 185.31 184.04 182.81 181.61 180.42
Alt. 706.61 705.84 705.19 704.87 704.86

Precursor's morphology shows their uniqueness permitting to separate them from other kinds of ionospheric variability

* Locality
* Time development
* Local time dependence
* Vertical profile modification
* Mean ion mass changes
* Plasma parameters changes (electron and ion temperatures, plasma instabilities, etc.)
* Specific EM emissions
* Particle precipitation
* Conjugancy and deep role; of the equatorial anomaly

ИКИ
ИНСТИТУТ
КОСМИЧЕСКИХ
ИССЛЕДОВАНИЙ
РАН

Different temporal evolution

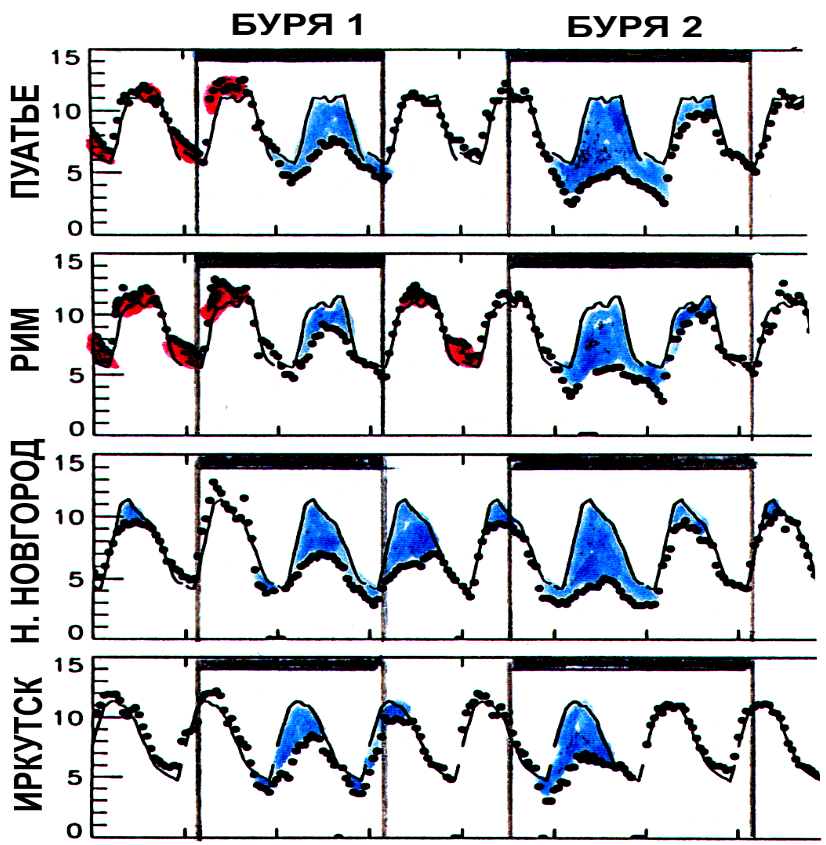

Chung Li ionosonde, Taiwan

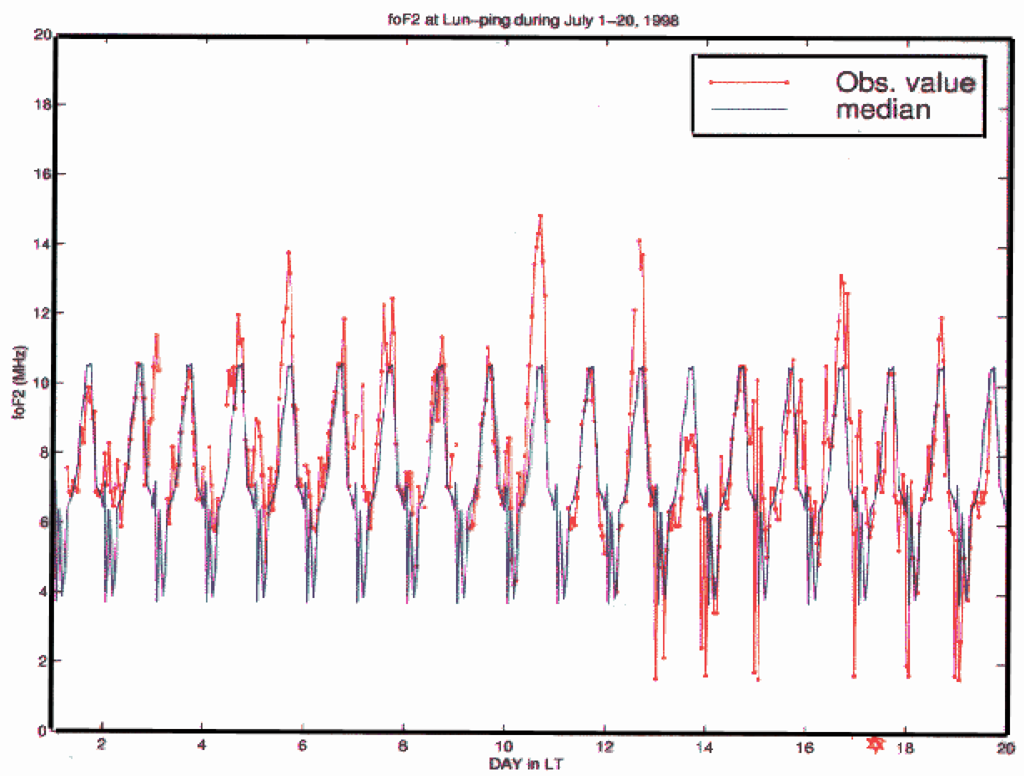

ИКИ
ИНСТИТУТ
КОСМИЧЕСКИХ
ИССЛЕДОВАНИЙ
РАН

Locality

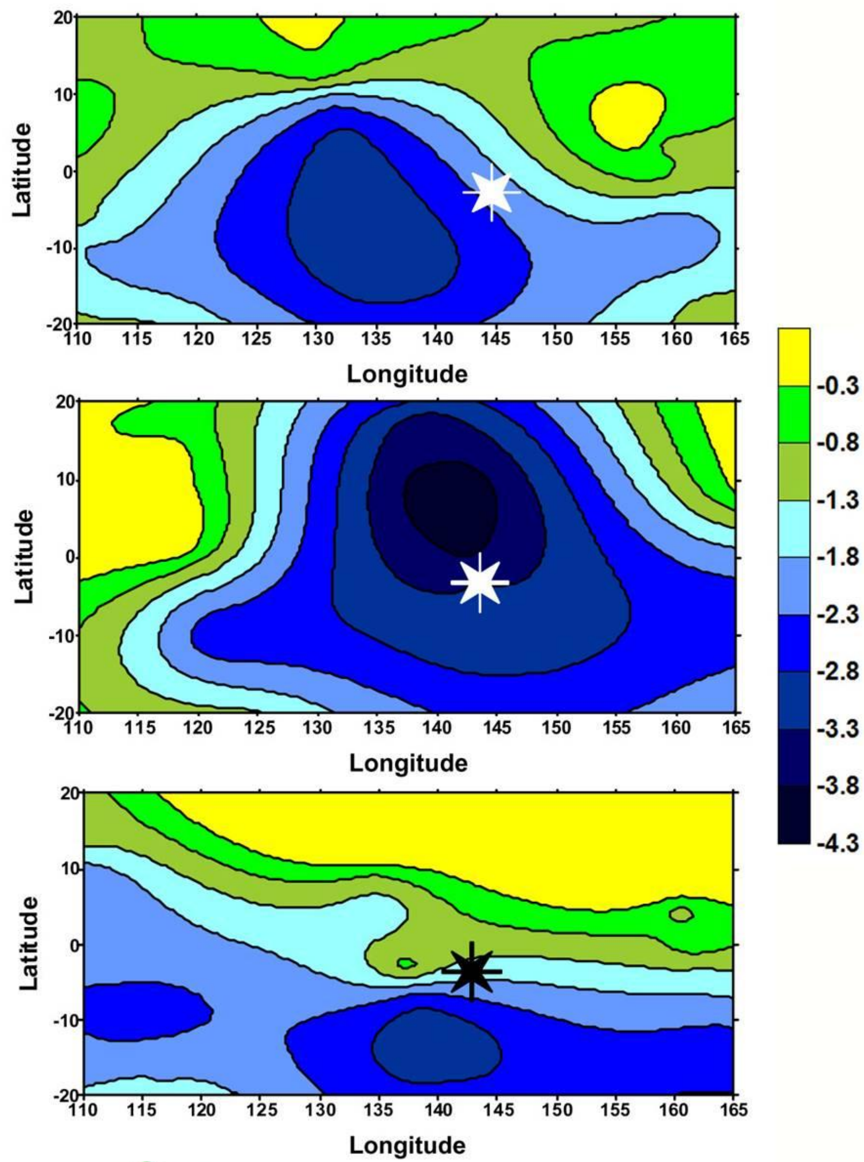

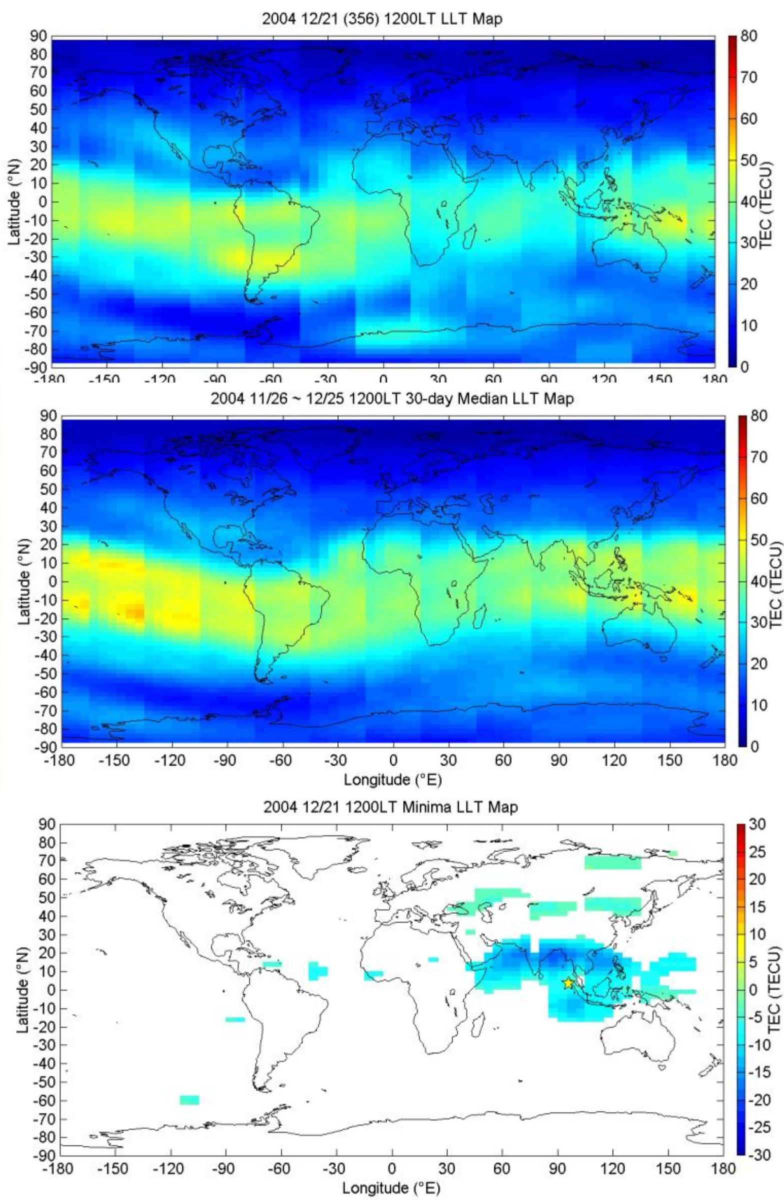

2004/12/21
(D-5)

2004/11/26
2004/12/25
30-day median

2004/11/26
2004/12/25
30-day minimum

ИКИ
ИНСТИТУТ КОСМИЧЕСКИХ ИССЛЕДОВАНИЙ РАН

Scale height effect in vertical profiles

$$N(z) = 4.0 * \frac{\exp\left(\frac{z}{B2u}\right)}{\left(1 + \exp\left(\frac{z}{B2u}\right)\right)^2}$$

where *B2u* characterizes the topside layer thickness and changes linearly with the height:

$B2_u = B_o + k \cdot z$, $\quad z = h - h_{max}$

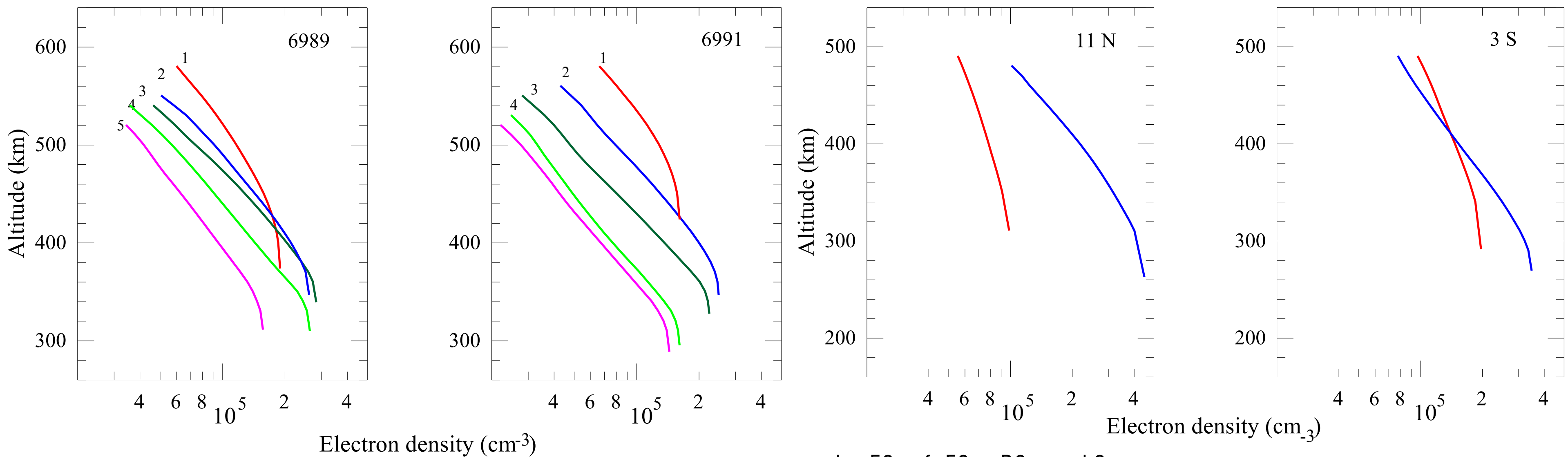

	lat	hmF2	foF2	B2u	k2u
1.	8.4	375	12.4	75.8	0.02
2.	0.6	345	14.6	47.1	0.14
3.	-3.3	340	15.2	43.3	0.13
4.	-7.2	310	14.6	44.4	0.12
5.	-15.1	310	11.3	46.5	0.15

	lat	hmF2	foF2	B2u	k2u
1.	9.6	425	11.5	61.7	0.17
2.	1.8	345	14.2	47.5	0.12
3.	-2.2	325	13.5	40.6	0.12
4.	-10.0	295	11.4	44.6	0.13
5.	-14.0	290	10.8	48.4	0.11

hmF2	foF2	B2u	k2u
260	6.0	54.0	0.16
320	2.8	87.0	0.29

	hmF2	foF2	B2u	k2u
7286	270	5.3	44.7	0.17
7301	290	4.0	69.0	0.26

Mean ion mass effect

$$H_s = \frac{T_e + T_i}{M_+ / 0.85 + (\frac{h}{R_0} + 1)^2 \frac{dT_e}{dh}}$$

R_0 - Earth radius

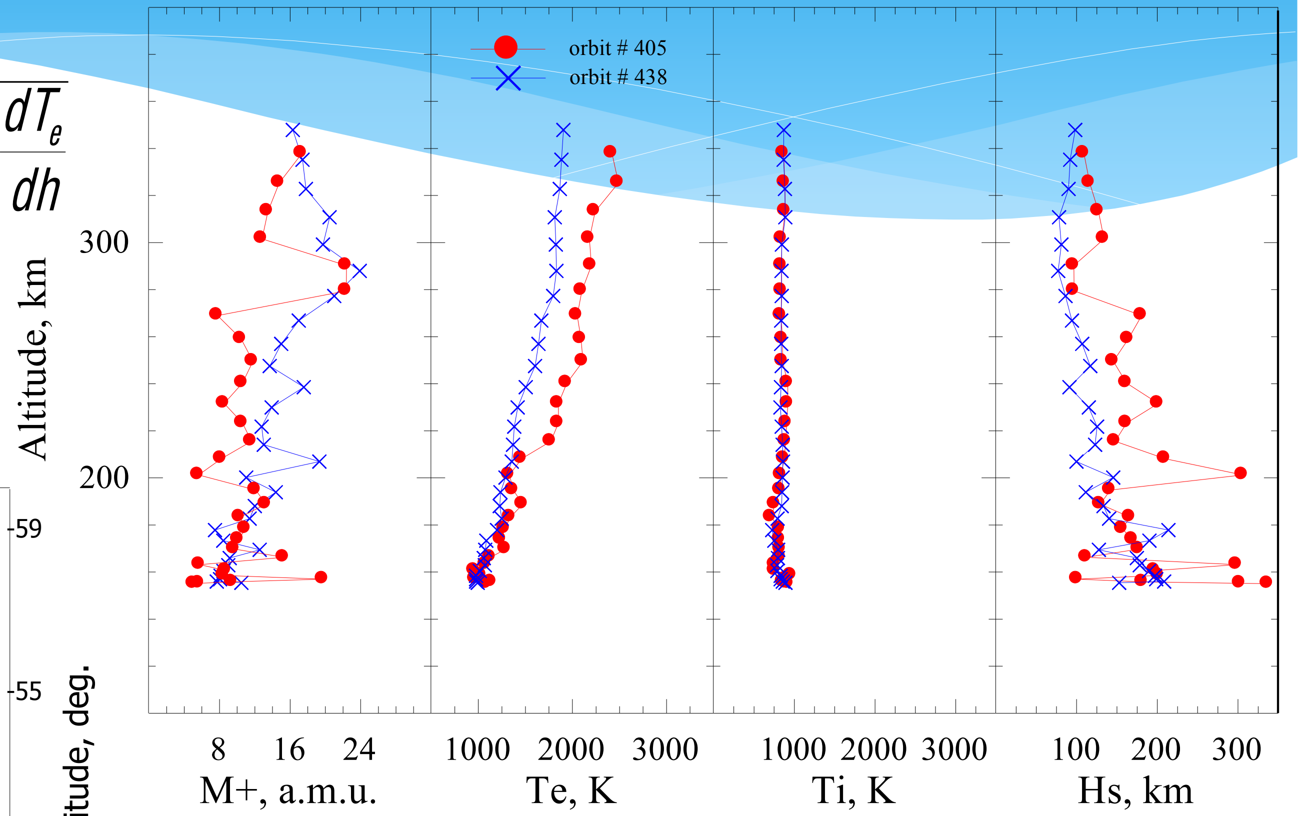

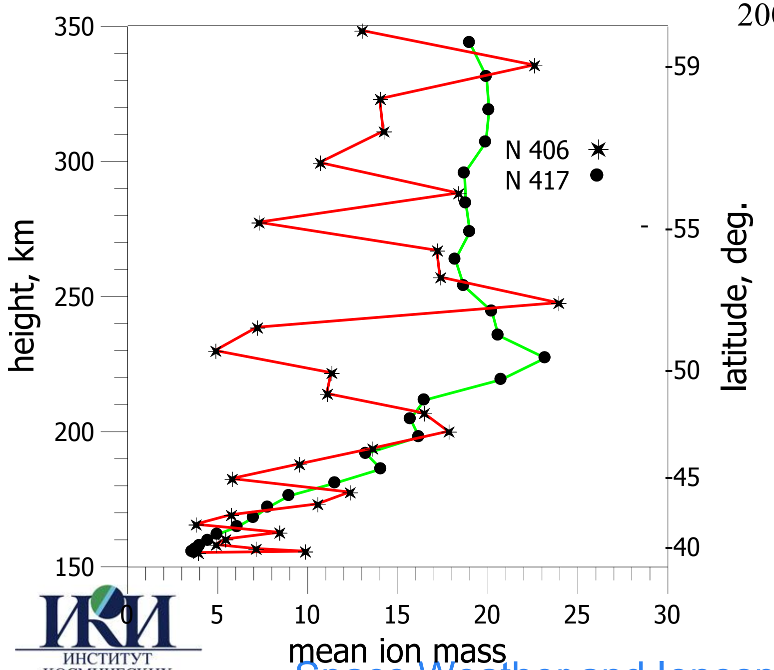

Irpinia earthquake M6.9 23 Nov 1980

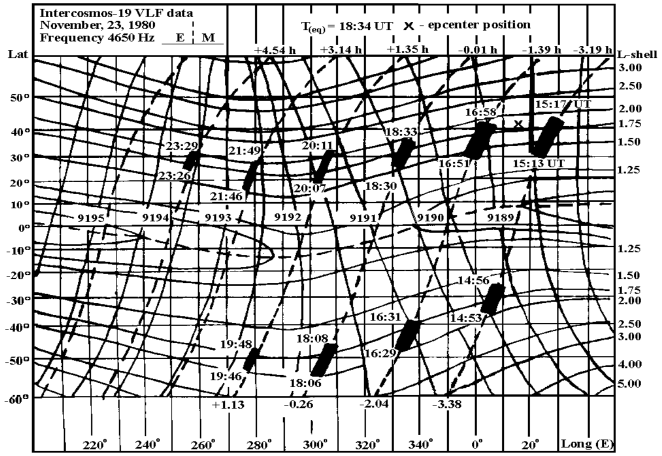

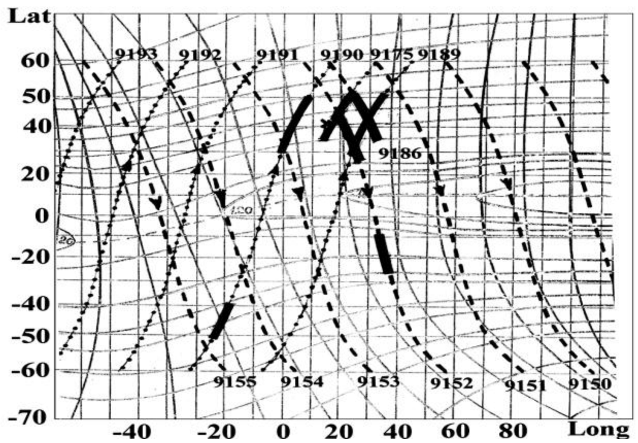

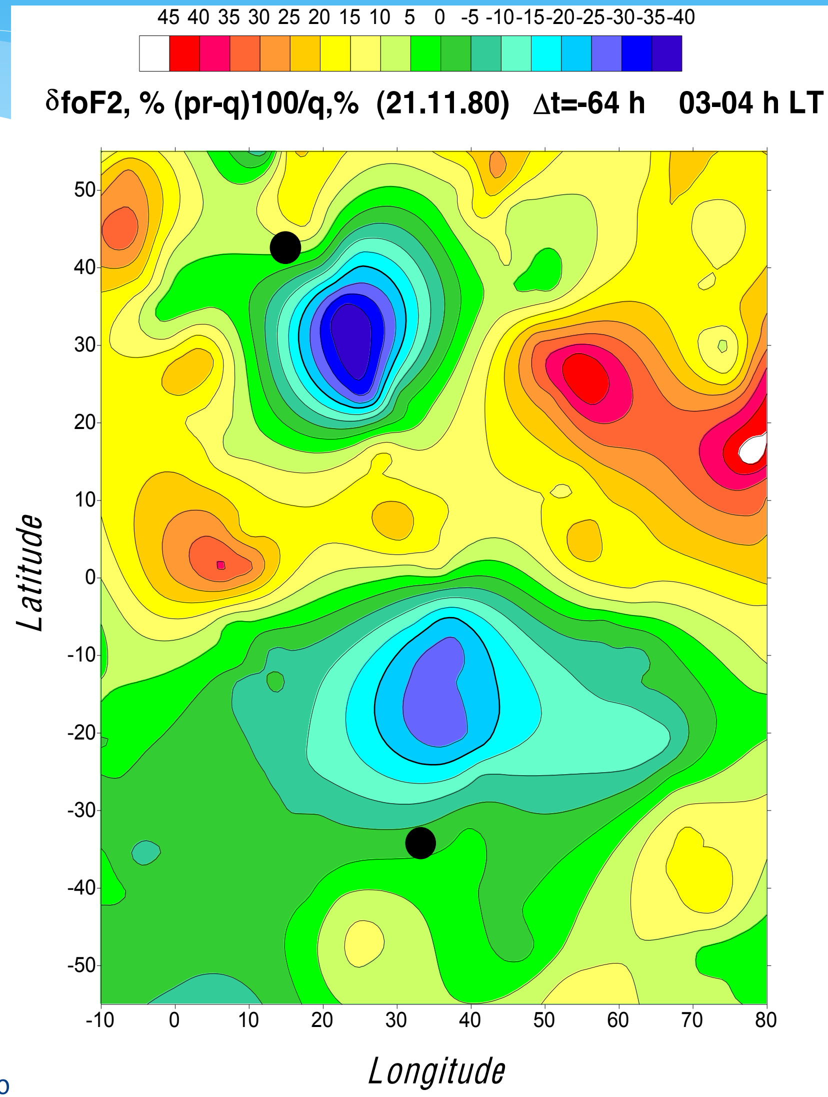

Modeling

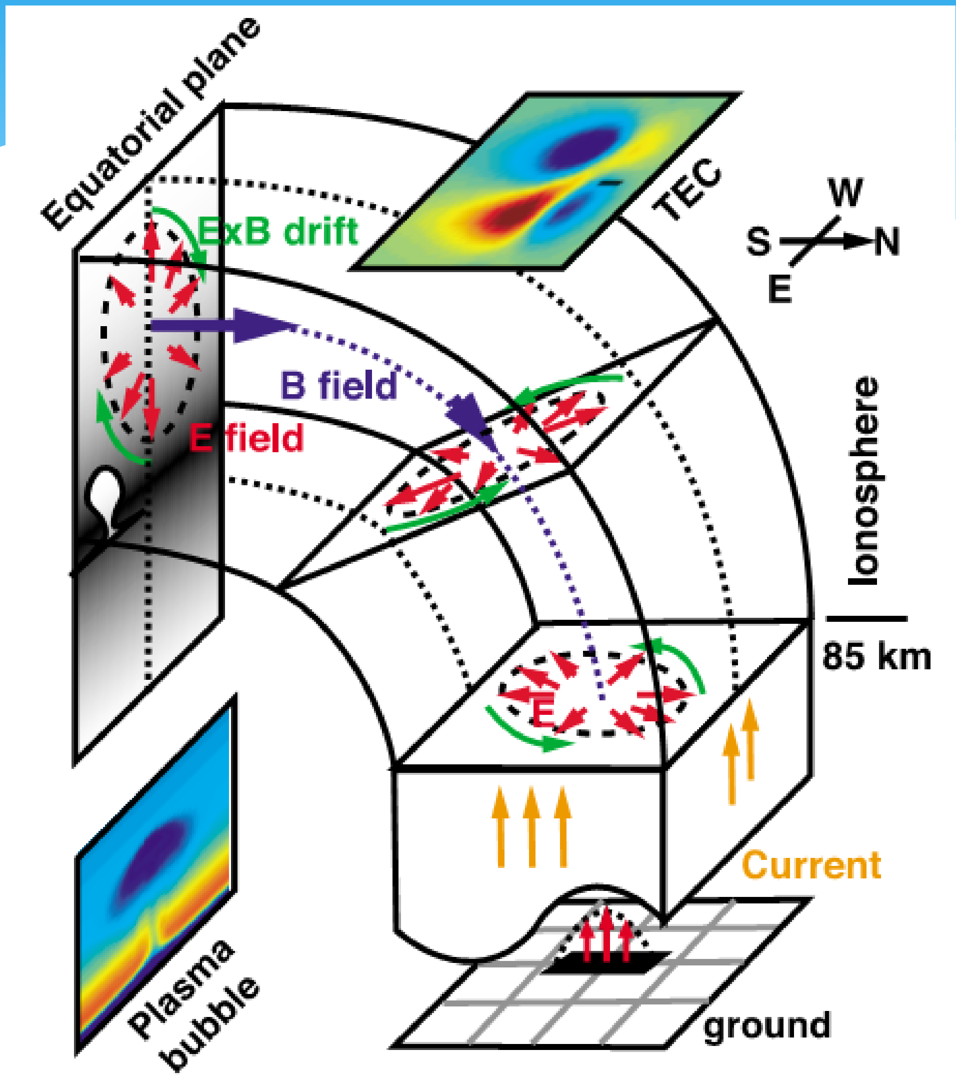

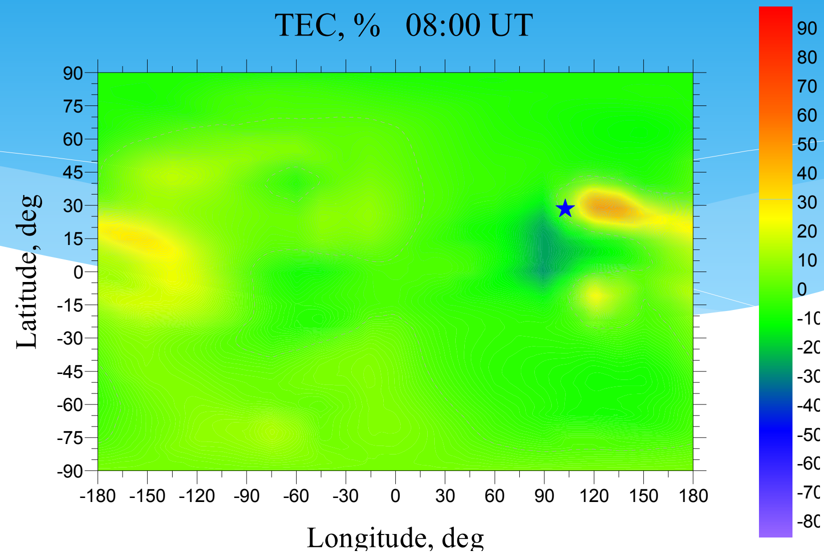

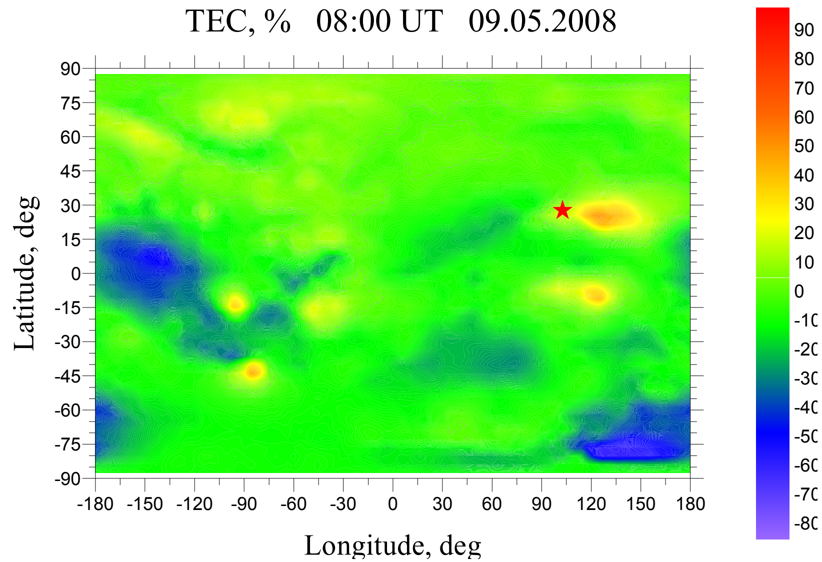

Kuo et al., JGR, 2011

Klimenko et al., ASR, 2011

Formal anomaly determination

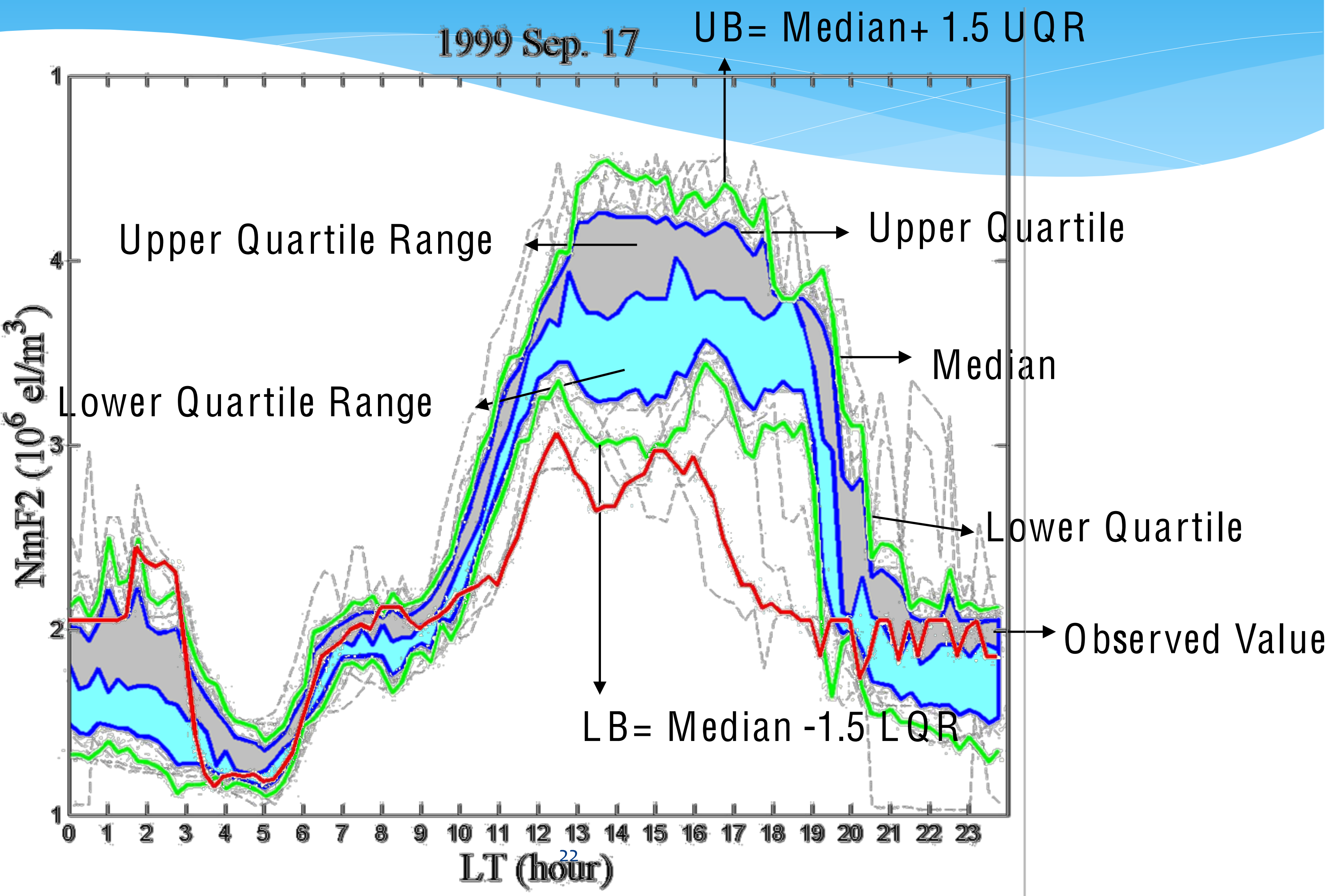

ИНСТИТУТ КОСМИЧЕСКИХ ИССЛЕДОВАНИЙ РАН

Statistics

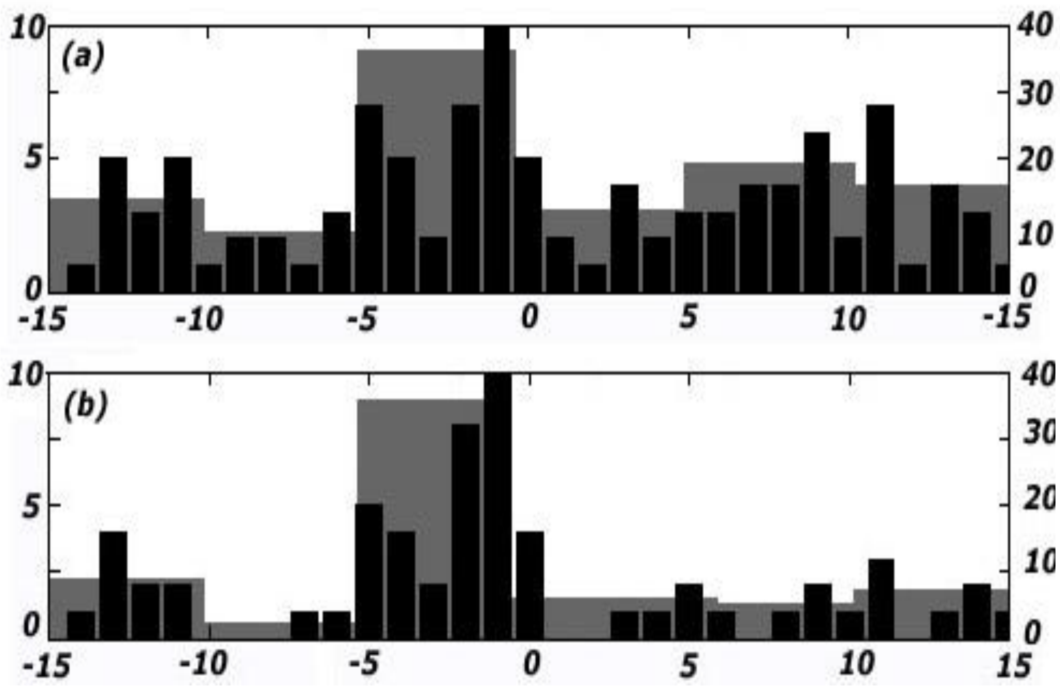

Liu et al. (AG 2004)

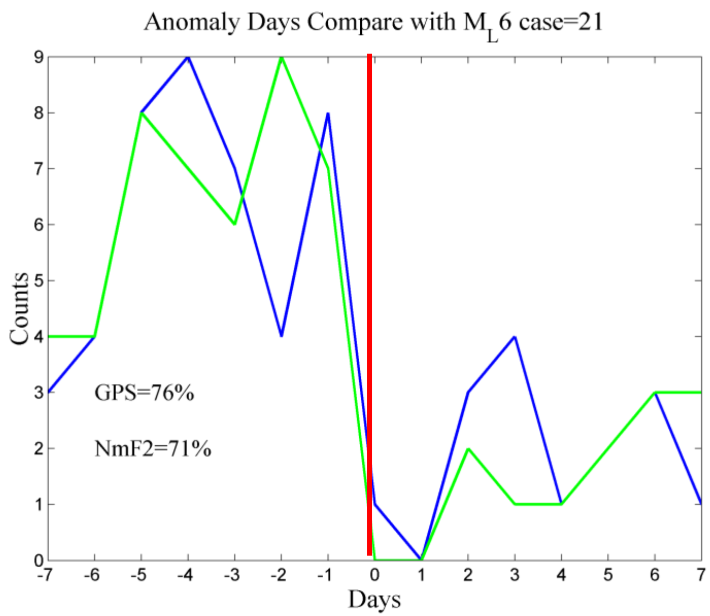

ИНСТИТУТ КОСМИЧЕСКИХ ИССЛЕДОВАНИЙ РАН

Main result of DEMETER satellite

EQ data

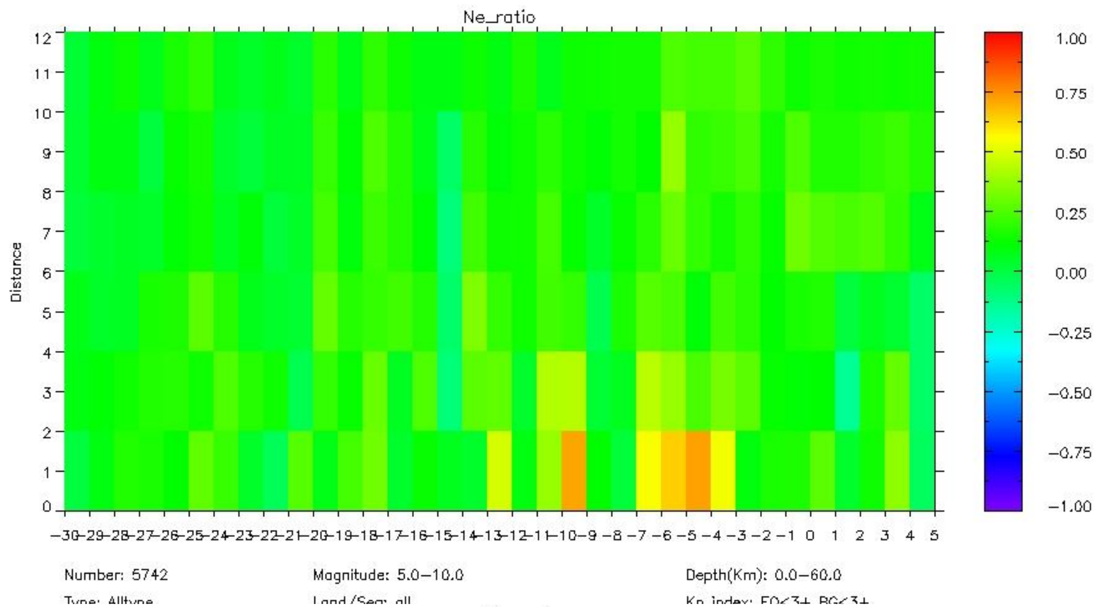

5742 EQ

Random data

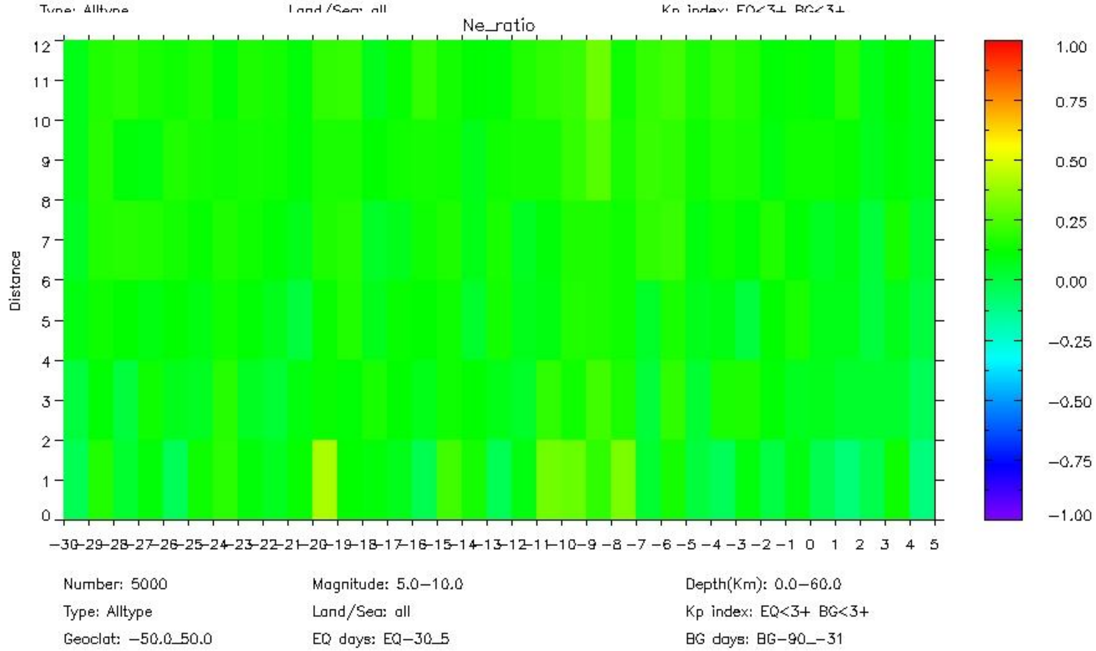

ИНСТИТУТ КОСМИЧЕСКИХ ИССЛЕДОВАНИЙ РАН

Haiti earthquake M7.9 Jan 12, 2010

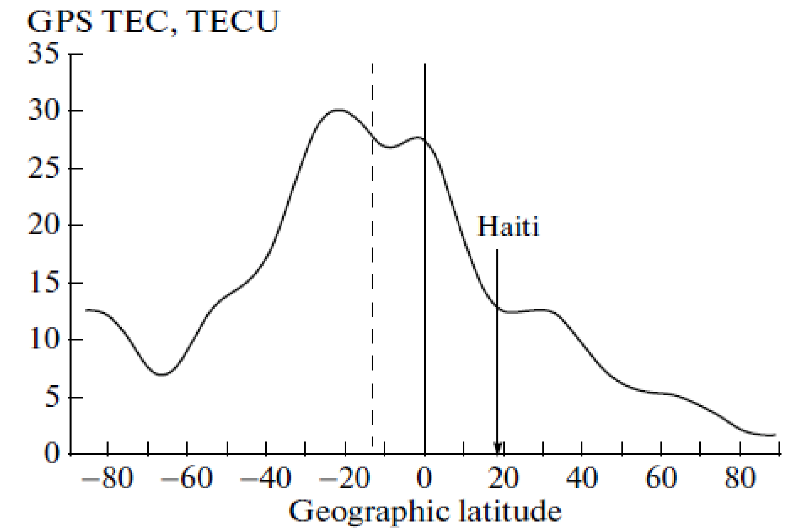

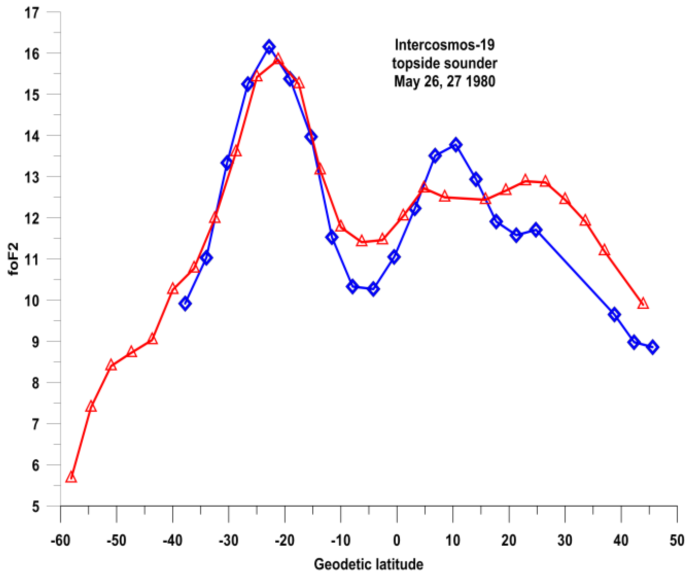

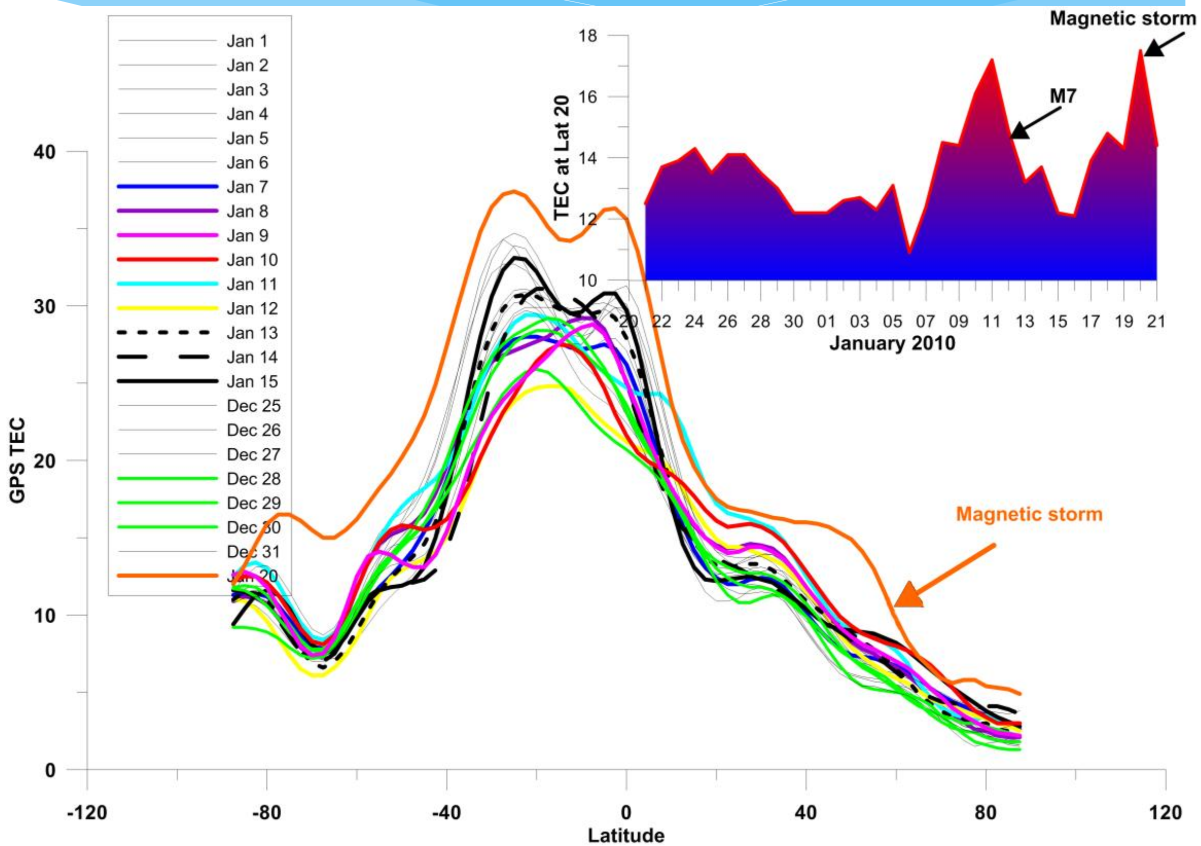

ИКИ
ИНСТИТУТ
КОСМИЧЕСКИХ
ИССЛЕДОВАНИЙ
РАН

Tohoku M9 earthquake March, 11, 2011 complex geophysical conditions

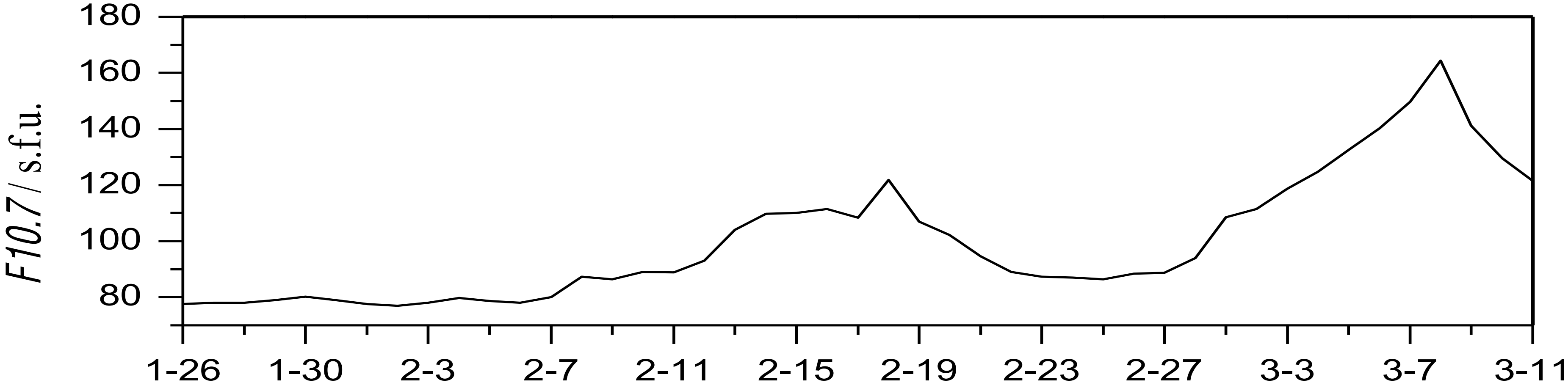

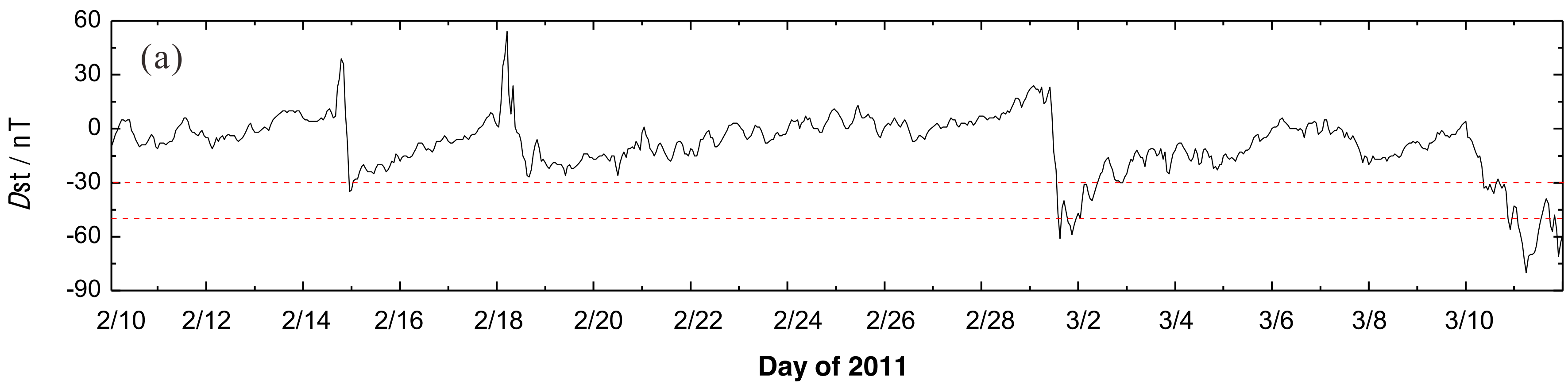

EQ effect separation from F10.7 and magnetic storm effects

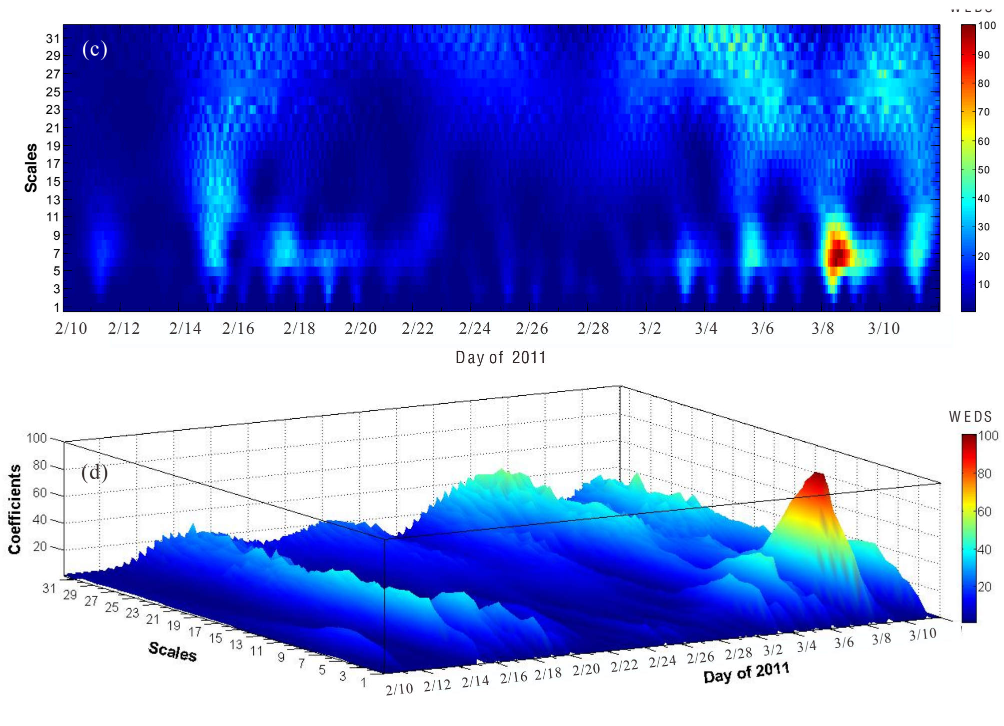

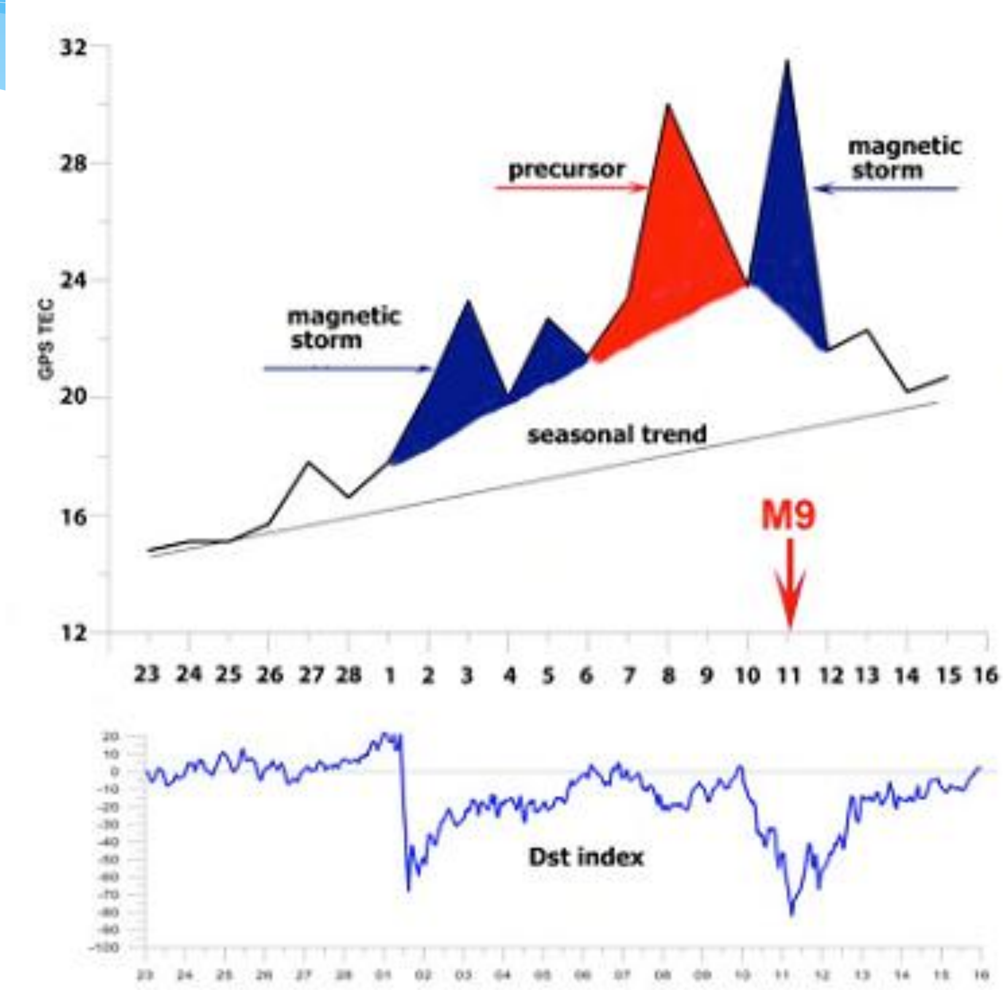

ИКИ
ИНСТИТУТ
КОСМИЧЕСКИХ
ИССЛЕДОВАНИЙ
РАН

Detection 1
Precursor mask conception

We represent the state of the ionosphere prior to the event in the form of an A_{ij} matrix whose columns contain the hourly deviations of *foF*2 from its median value. The number of columns in the matrix is determined by an expected time interval between a precursor and an event. In this paper, we assume that this interval does not exceed six days and, respectively, the dimension of the A_{ij} matrix is 24×6, i.e., $i = 1 \ldots 24$, $j = 1 \ldots 6$.

For all events we form matrices in the same manner and obtain an $A_{ij}^{(n)}$ series, where n is the ordinal number of an event. We now introduce the value

$$S_n = \frac{\sum\limits_{i,j} \langle A_{ij}^{(n)} \rangle_n^2}{\langle \sum\limits_{i,j} (A_{ij}^{(n)})^2 \rangle_n},$$

where $\langle \ldots \rangle_n$ means averaging over an ensemble of n events. S_n is the dispersion normalized so that $S_1 = 1$.

With the help of S_n, it is convenient to characterize the degree of $A_{ij}^{(n)}$ similarity at various n. For example, if $A_{ij}^{(n)}$ values for various events do not correlate with one another, the S_n series tends to unity at $n \longrightarrow \infty$. In the other extreme case, when the states of the ionosphere prior to all events are completely identical, S_n increases: $S_n \sim n$ at $n \longrightarrow \infty$.

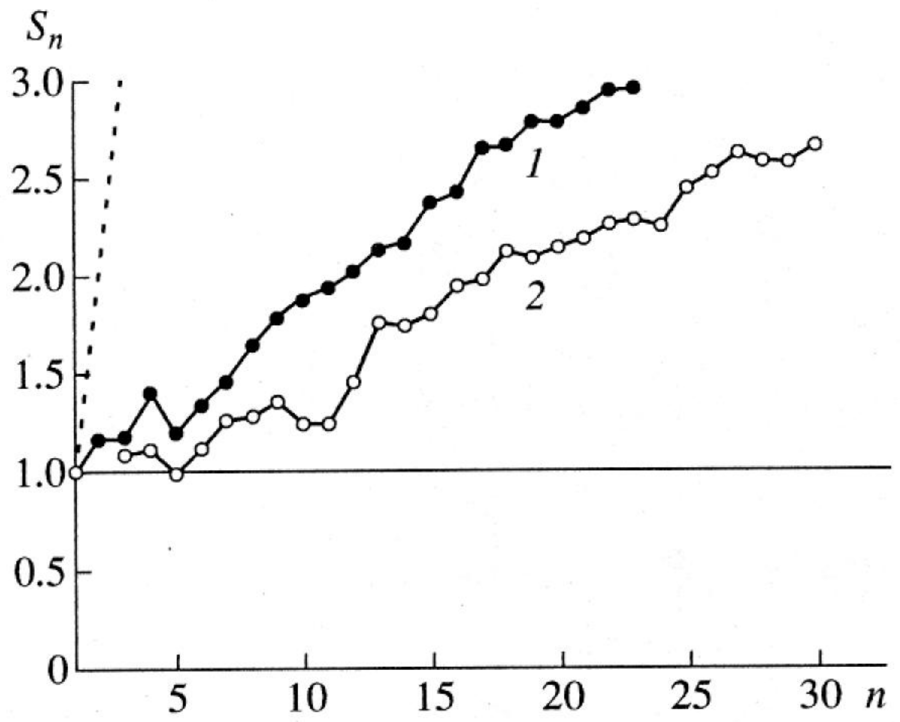

Fig. 2. Behavior of the S_n parameter for two groups of deep-focus earthquakes: a series of 23 (curve *1*) and 30 (curve *2*) events. Dashed and solid curves: theoretical curves for a similar state and noncorrelated states of the ionosphere prior to any earthquake in the series, respectively.

ИКИ
ИНСТИТУТ КОСМИЧЕСКИХ ИССЛЕДОВАНИЙ РАН

Mask for GPS TEC precursors at Taiwan

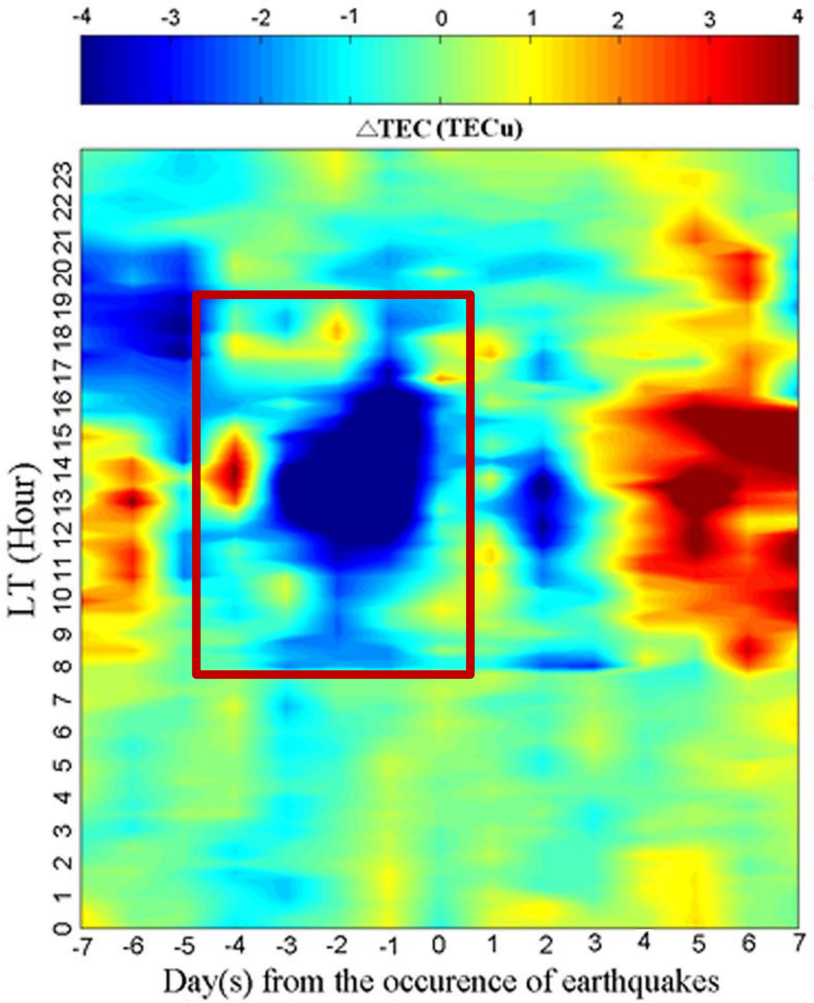

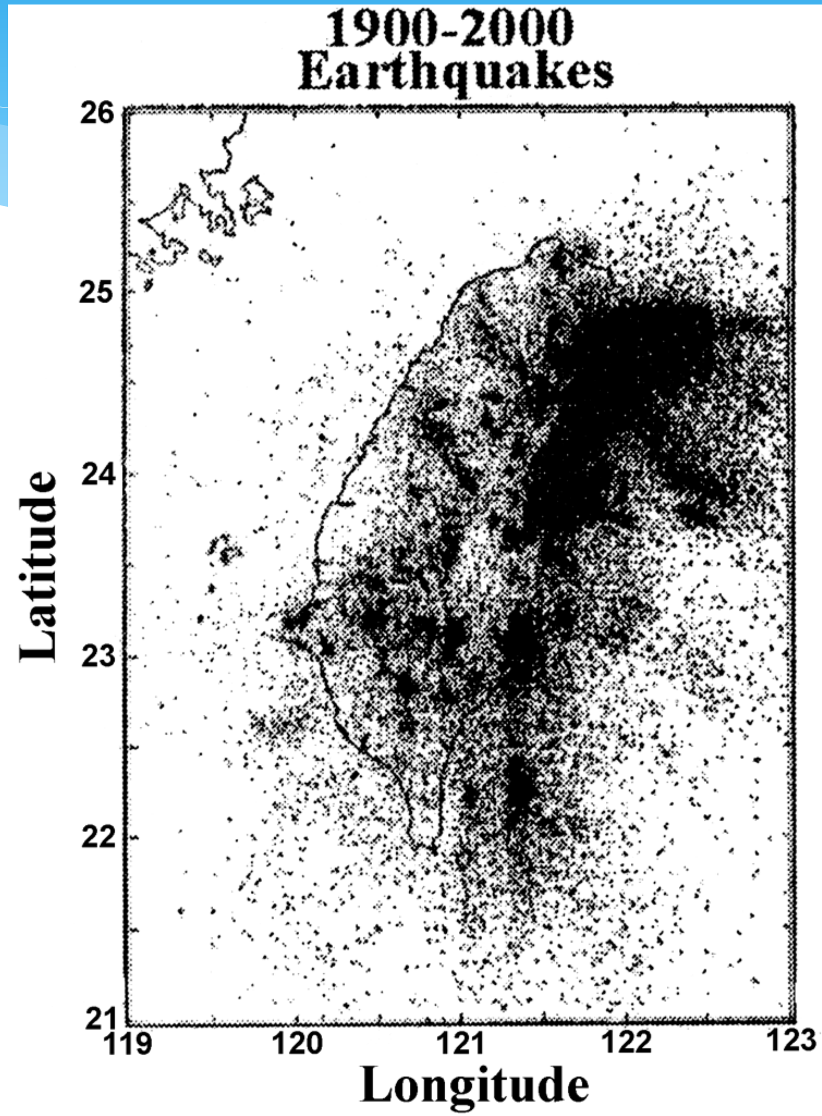

ИКИ
ИНСТИТУТ КОСМИЧЕСКИХ ИССЛЕДОВАНИЙ РАН

Cross-correlation coefficient

$$C = \frac{\sum_{i=0,k} (f_{1,i} - af_1)(f_{2,i} - af_2)}{k(\sigma_1 \sigma_2)}$$

$$af = \frac{\sum_{i=0,k} f_i}{k+1}$$

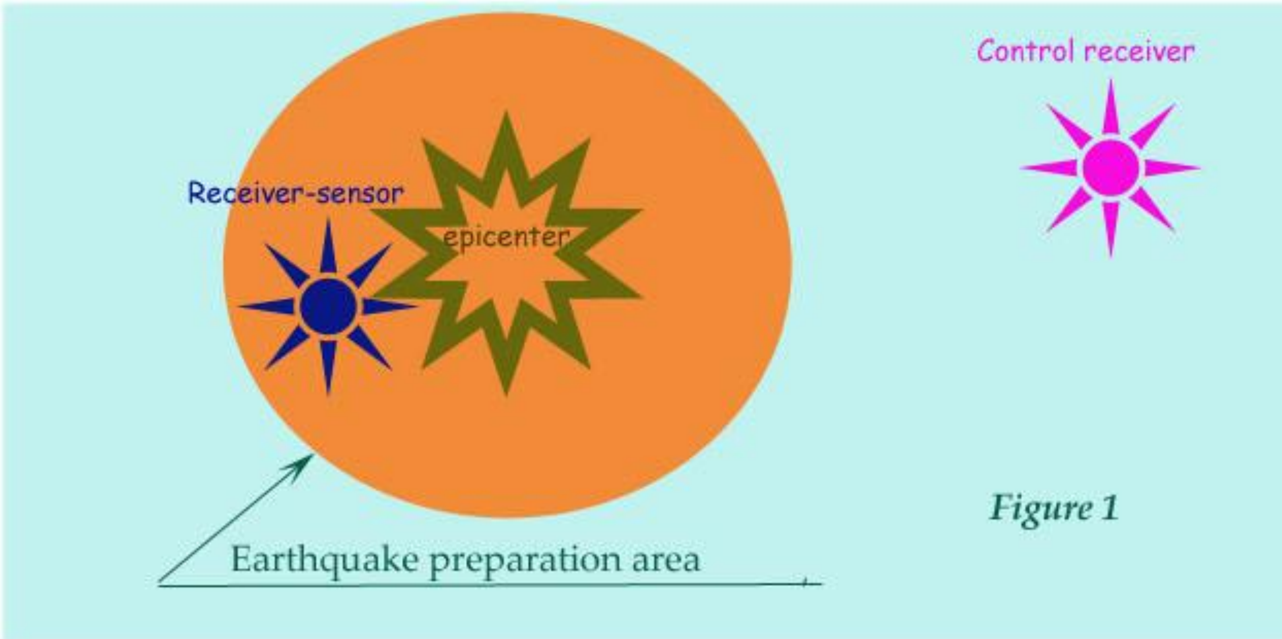

ИНСТИТУТ КОСМИЧЕСКИХ ИССЛЕДОВАНИЙ РАН

Examples of Cross-correlation

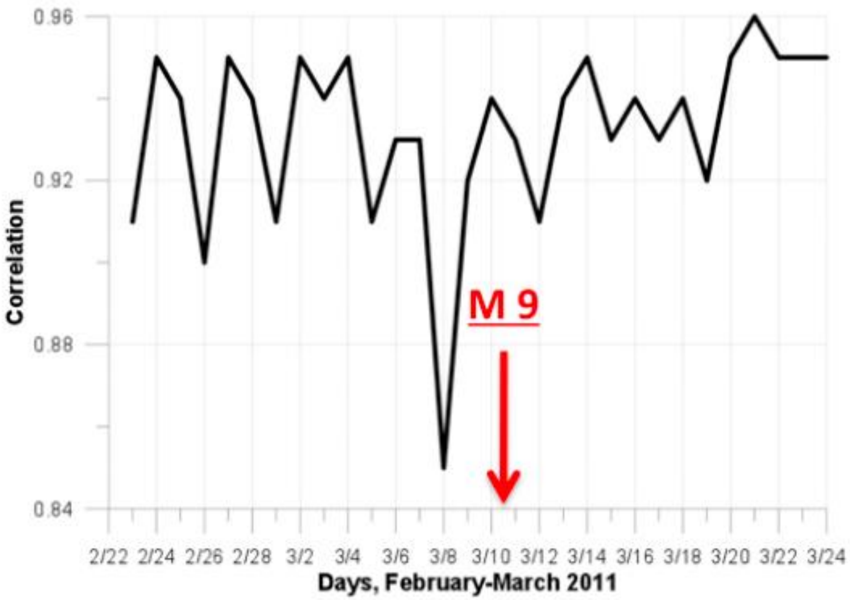

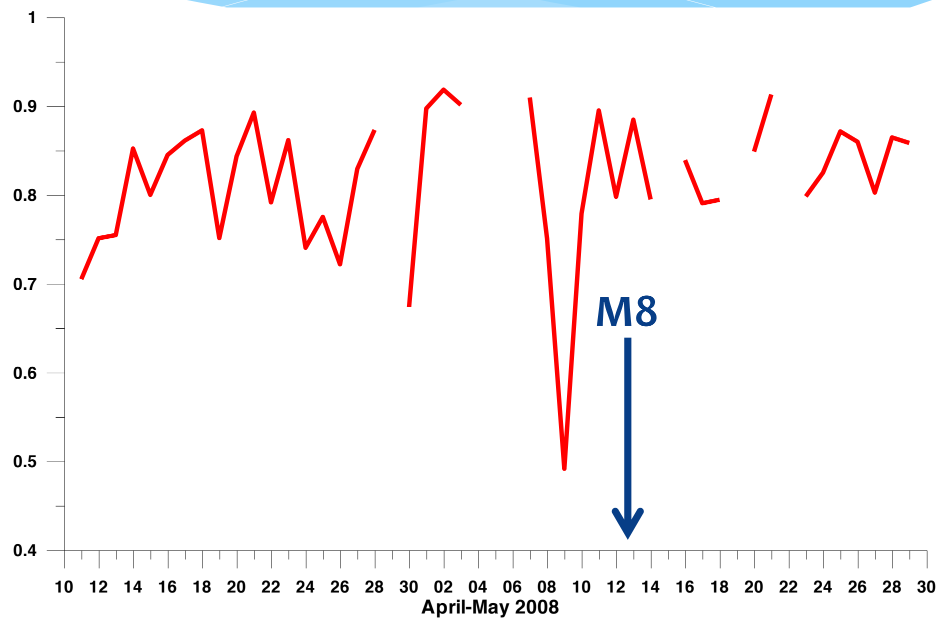

Tohoku EQ
Ionosondes
Kokubunji-Yamagawa

Wenchuan EQ
GPS receivers
kunm-shao

ИНСТИТУТ КОСМИЧЕСКИХ ИССЛЕДОВАНИЙ РАН

Local Variability Index

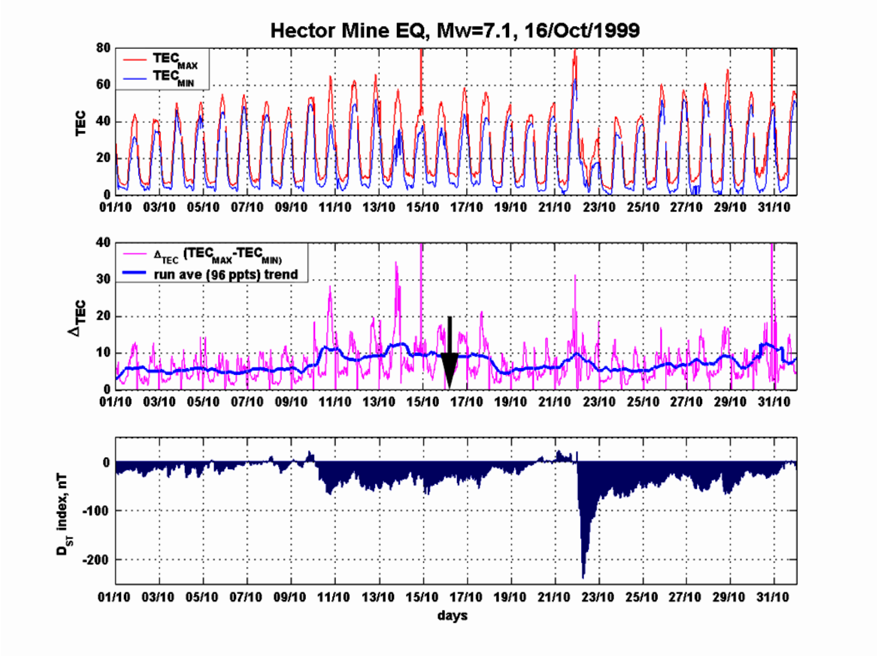

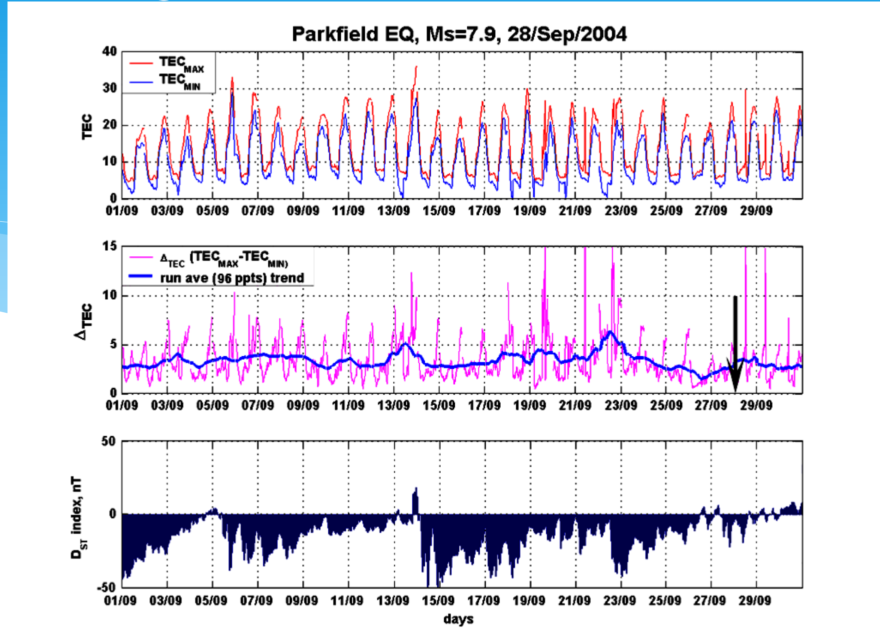

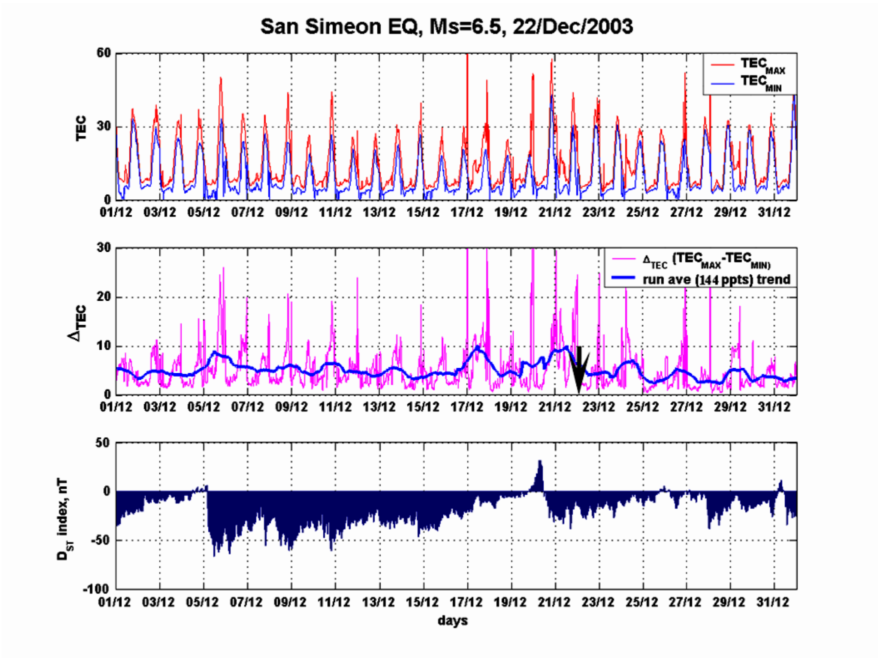

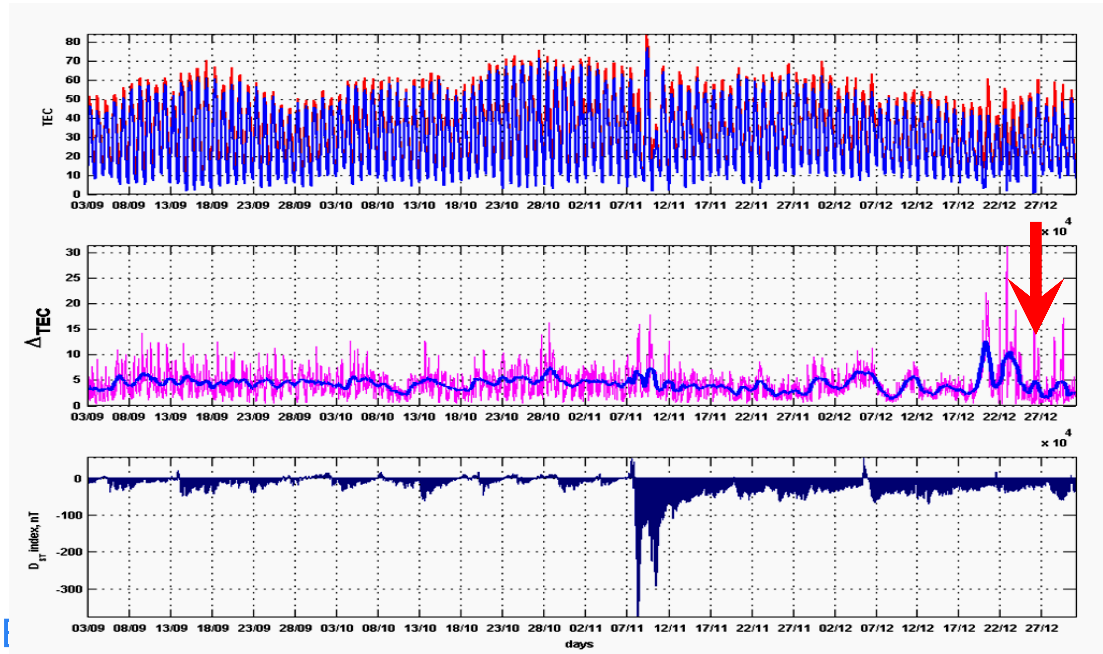

Regional TEC

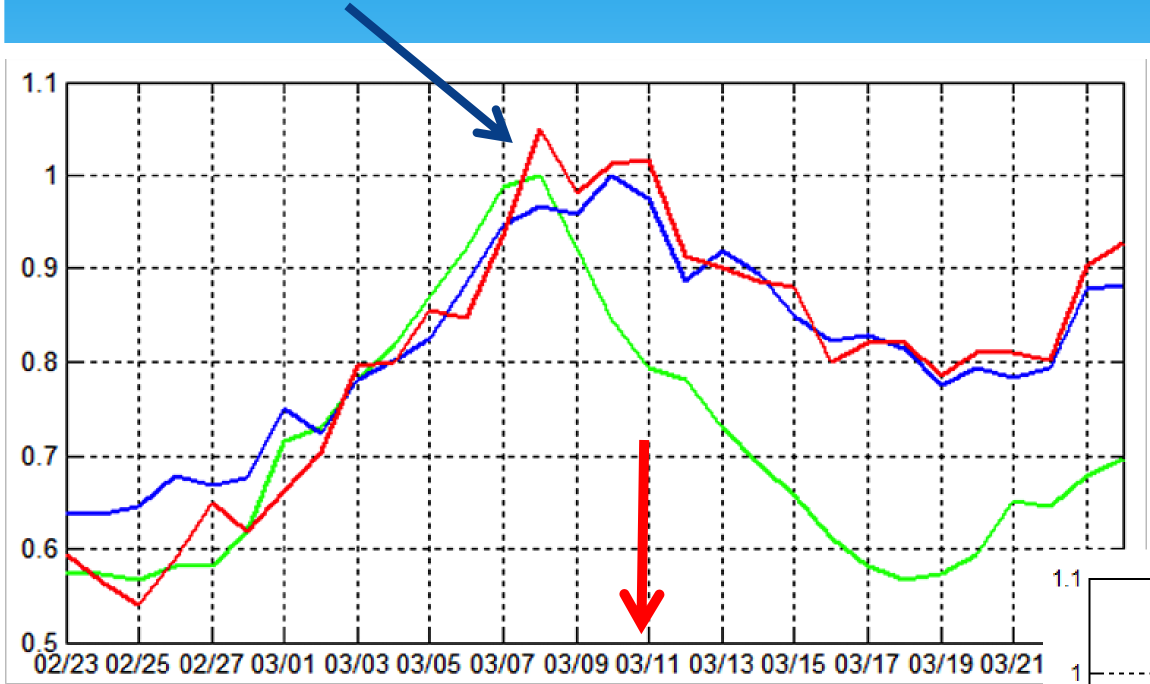

Tohoku earthquake
M9, 11 Mar 2011

Van earthquake
M7.2, 23 Oct 2011

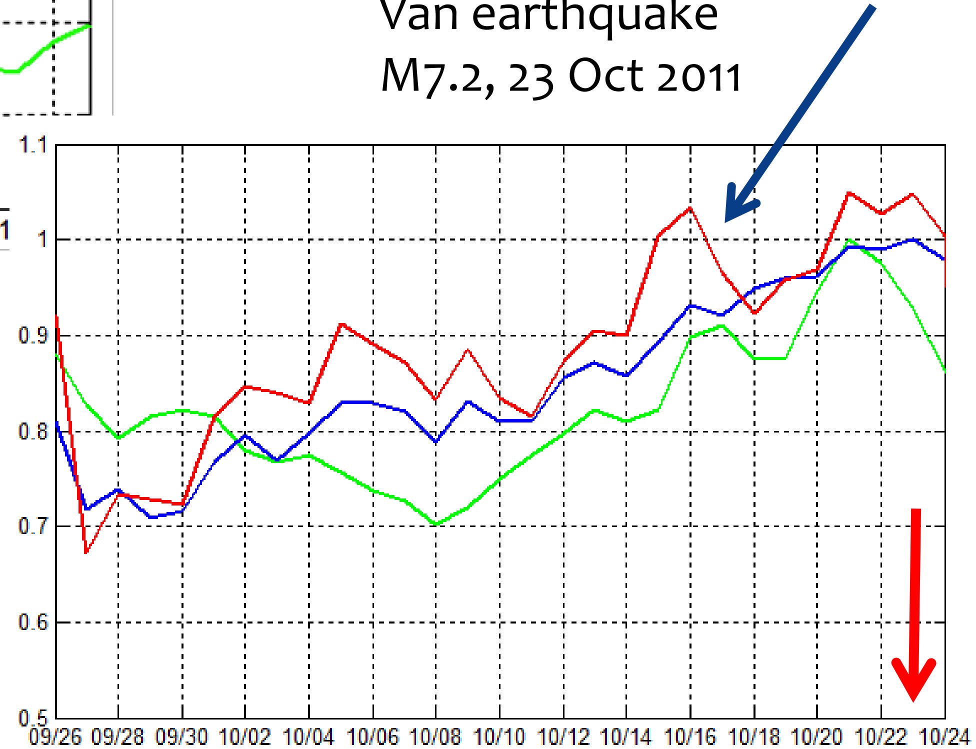

ИКИ
ИНСТИТУТ КОСМИЧЕСКИХ ИССЛЕДОВАНИЙ РАН

Sometimes Global TEC does not work

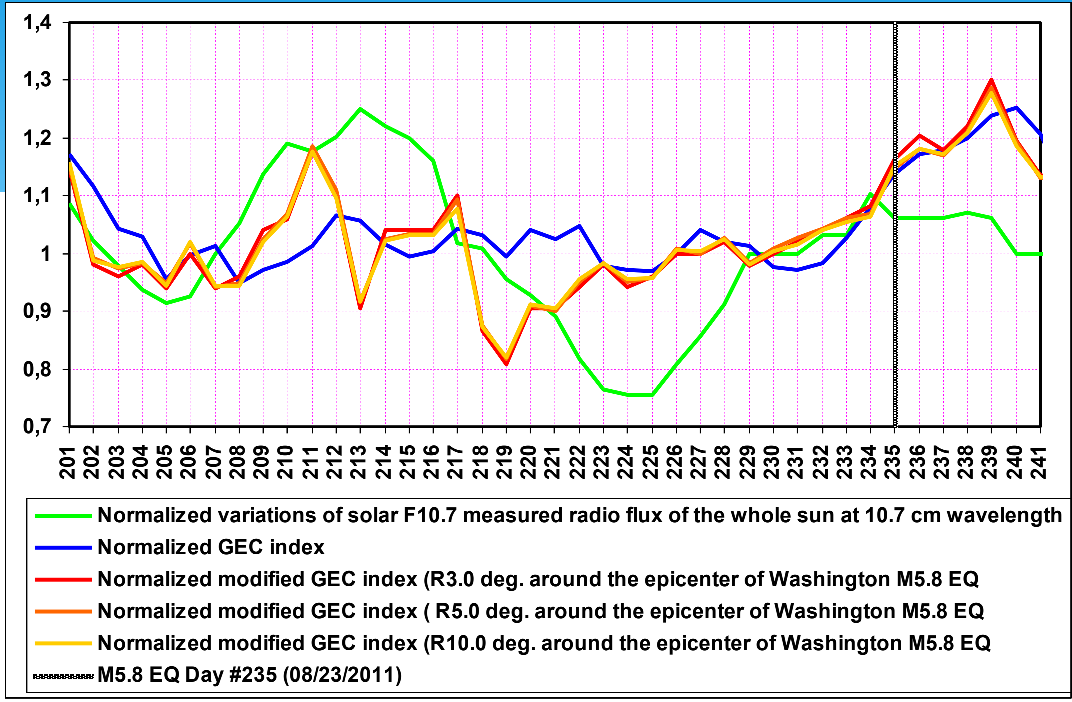

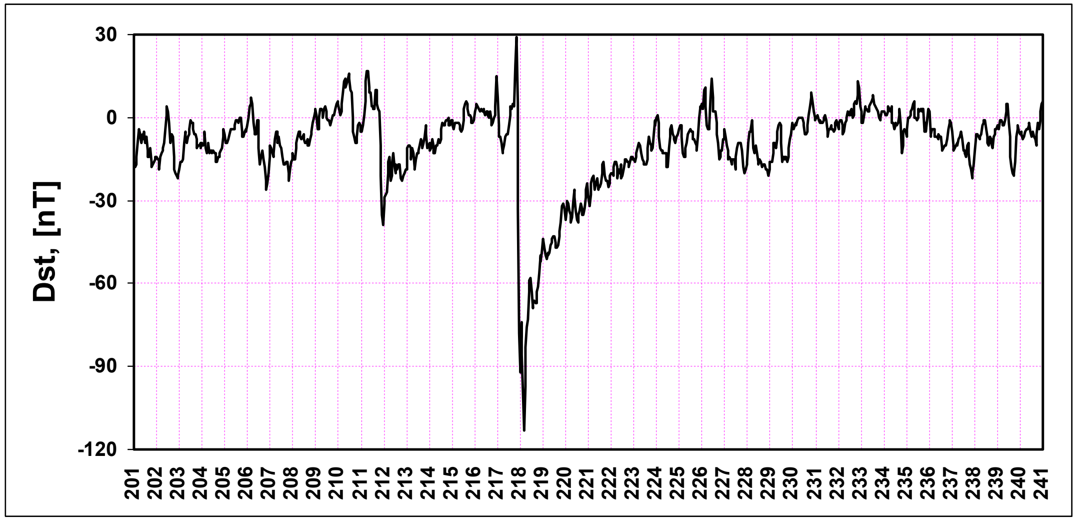

ИКИ
ИНСТИТУТ КОСМИЧЕСКИХ ИССЛЕДОВАНИЙ РАН

Ionospheric effects are part of complex LAIC conception

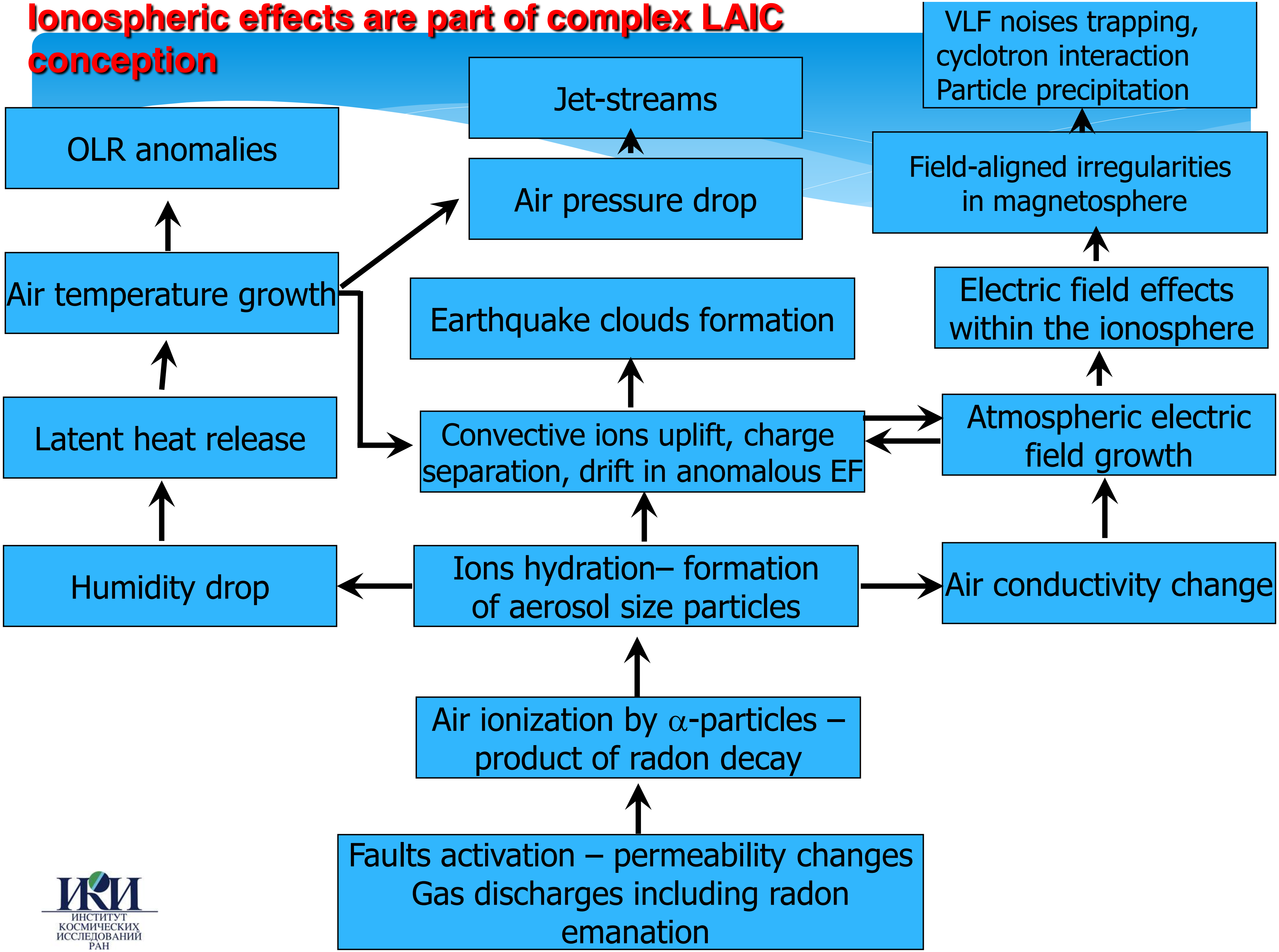

ИКИ
ИНСТИТУТ КОСМИЧЕСКИХ ИССЛЕДОВАНИЙ РАН

Two main branches of the LAIC model

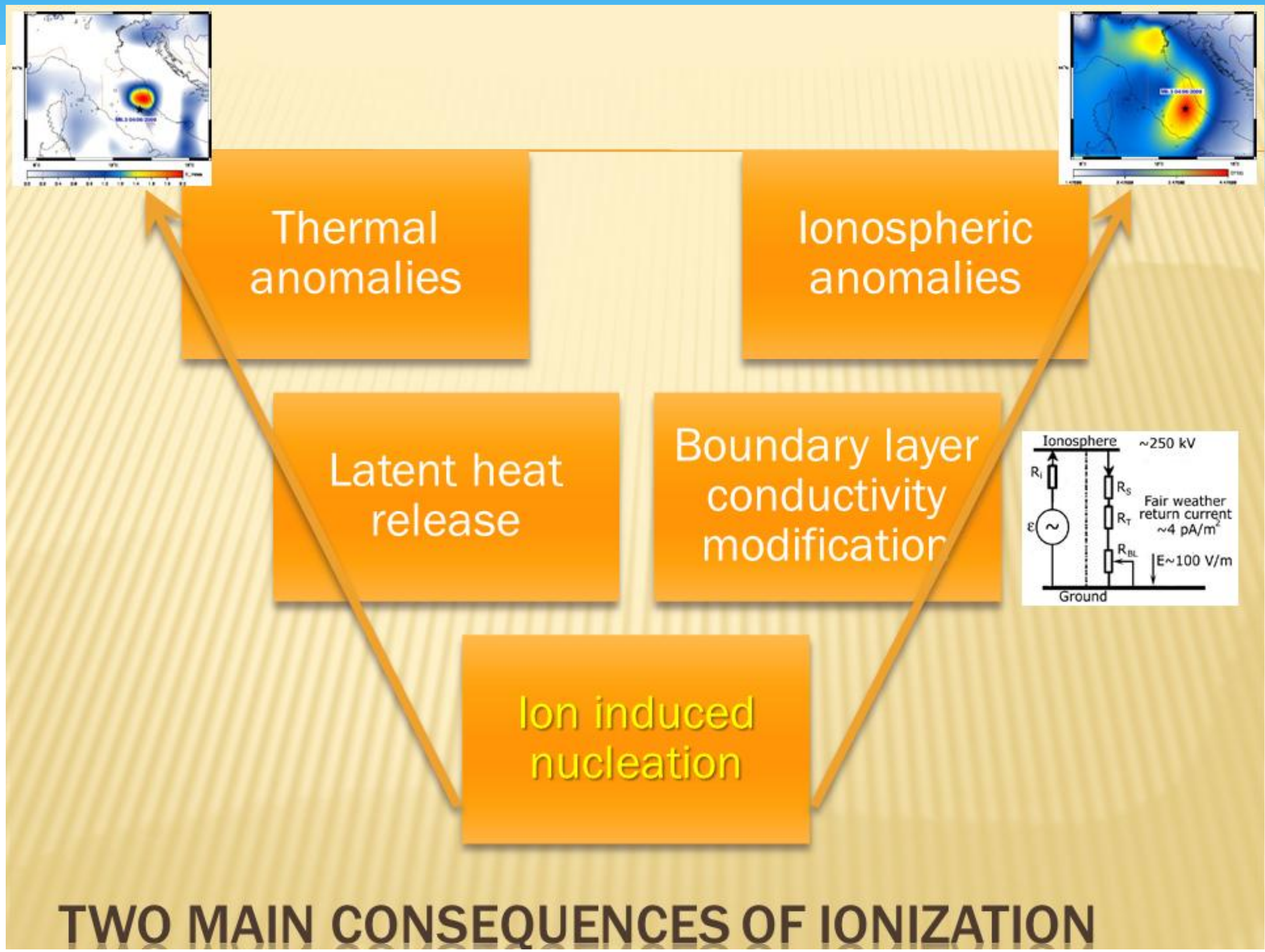

The synergy of earthquake precursors

l'Aquila, Italy, 06.04.2009

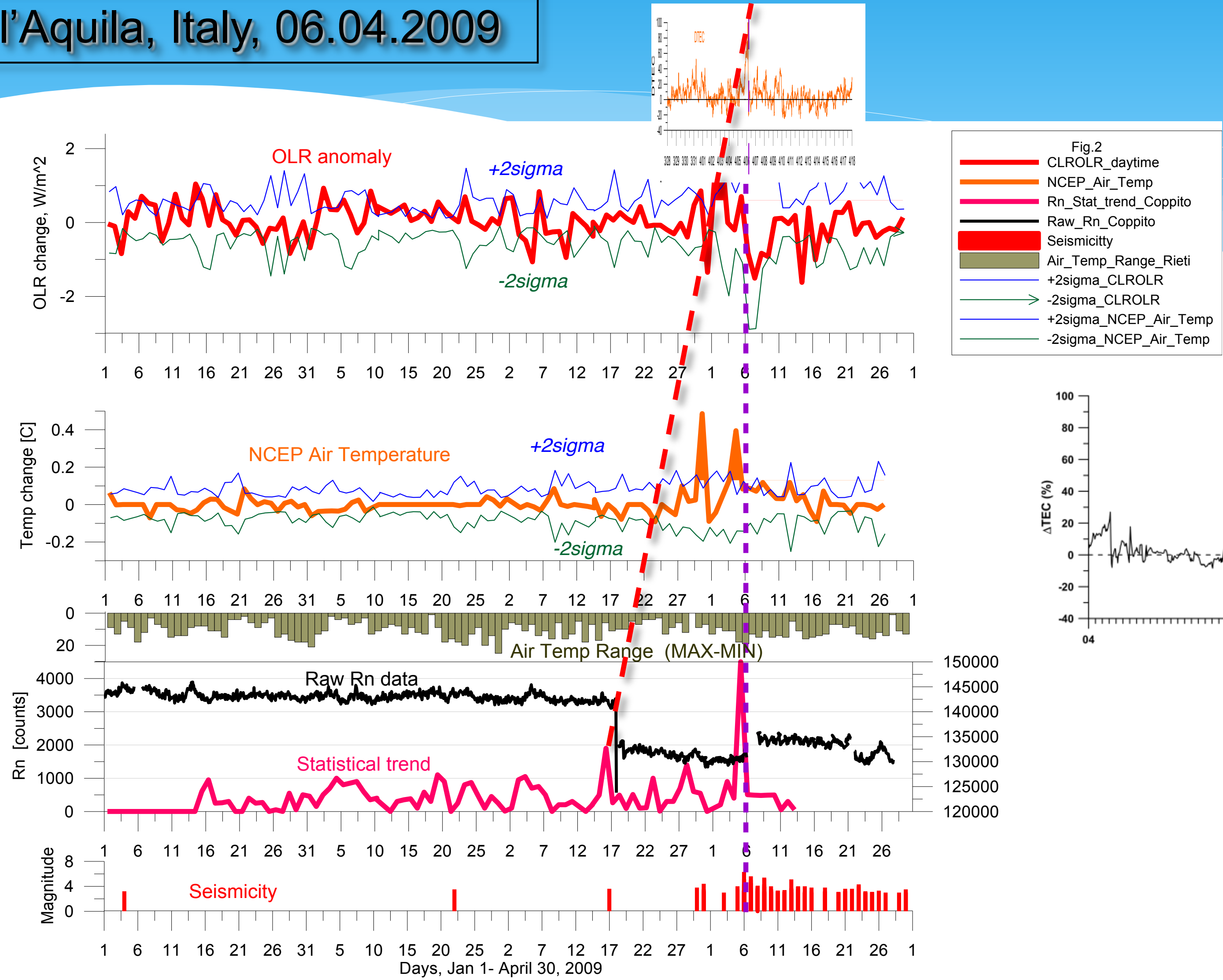

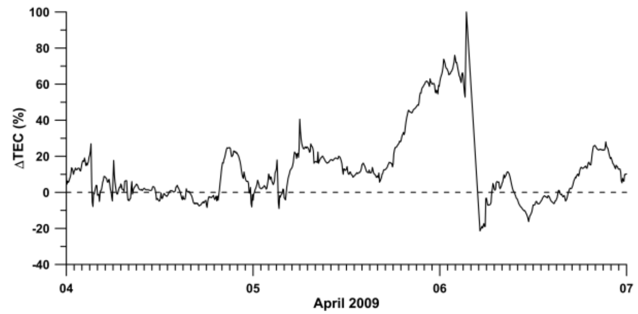

L'Aquila, Italy, 06.04.2009

OLR Anomaly

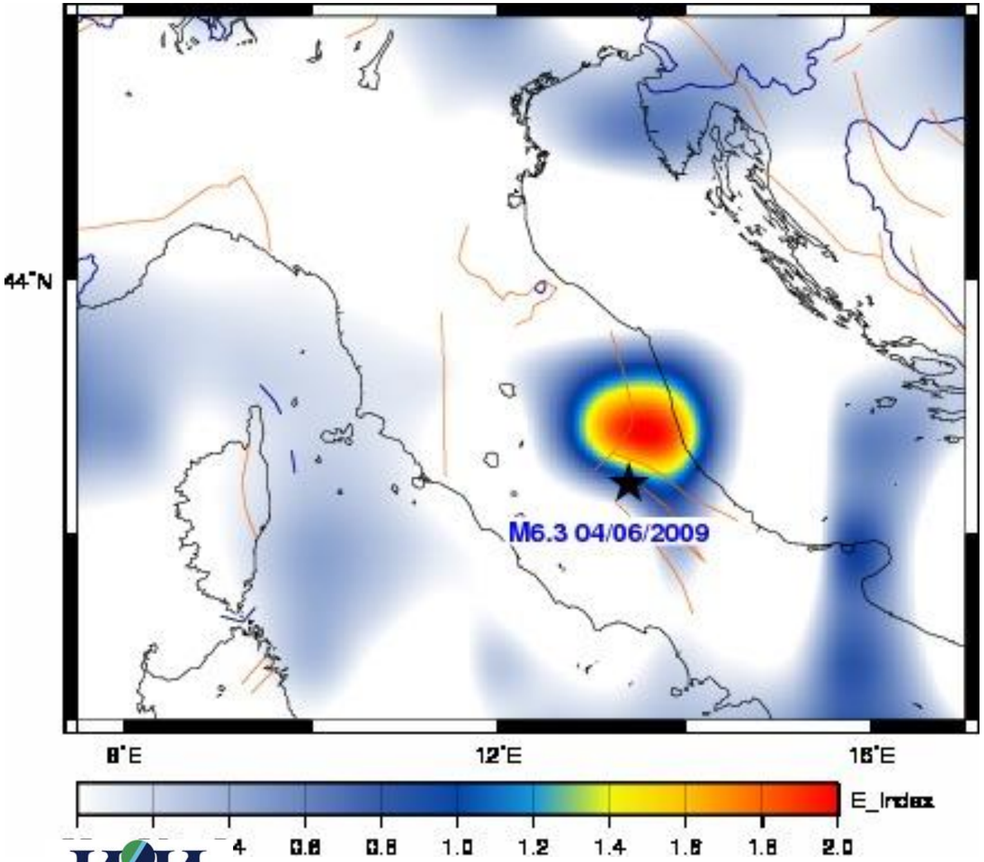

Ionospheric anomaly

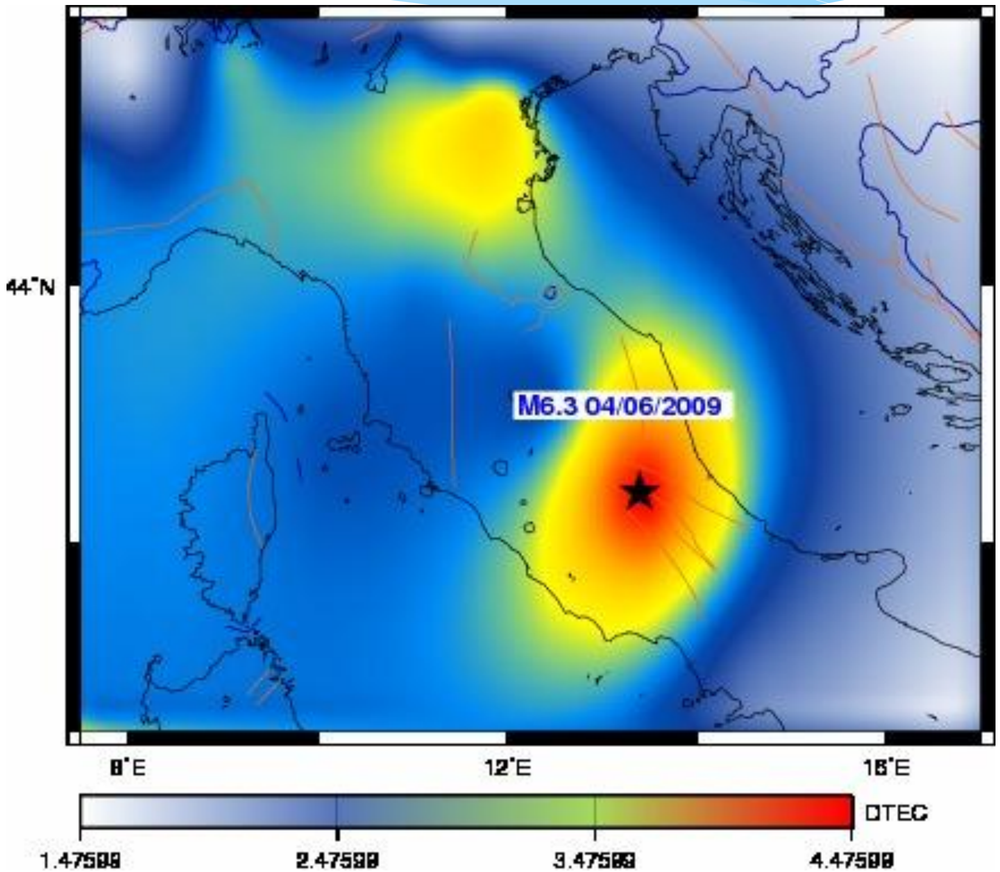

ИНСТИТУТ КОСМИЧЕСКИХ ИССЛЕДОВАНИЙ РАН

(Left) Day time OLR anomalous map for March 11 @7.30 LT, 2011 over Japan. (Middle) GPS/TEC Tomography March 11, (Right) Observed and predicted GPS displacements (GPS by the Caltech-JPL ARIA group}

Thermal map at TOA (-6 hours)

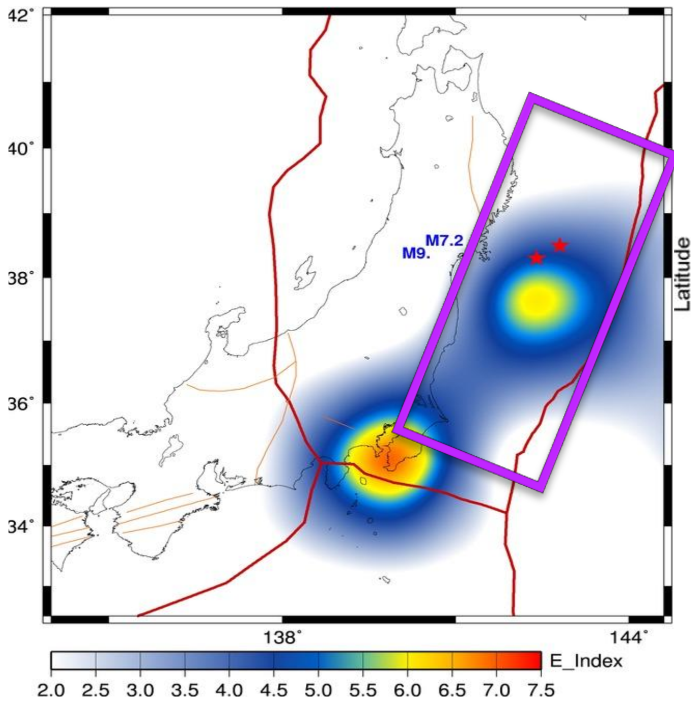

(Ouzounov et al, 2011)

TEC Tomography (-5 hours)

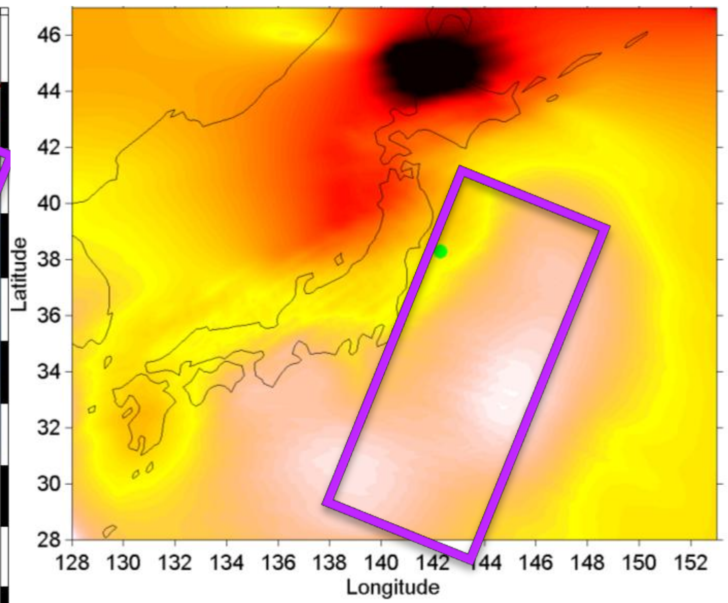

(Kunitzyn et al, 2011)

GPS Displacement

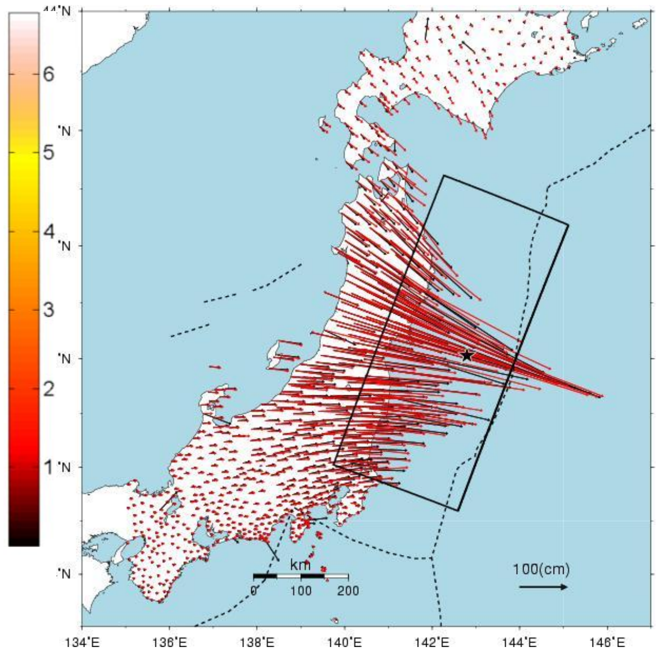

(Caltech/JPLARIA group)

ИНСТИТУТ КОСМИЧЕСКИХ ИССЛЕДОВАНИЙ РАН

Conclusions

* Ionospheric pre-earthquake effects are real, confident and physically grounded
* GNSS can be powerful instrument for the global detection of ionospheric precursors
* More ionospheric parameters are necessary for reliable identification of ionospheric precursors
* Ionospheric effects are part of more complex system of the Lithosphere-Atmosphere-Ionosphere Coupling
* The modern state of GPS TEC technology is able to provide the real time global monitoring of ionospheric precursors

Conclusions 2

* Regardless very dense network of GPS receivers, they undergo the same limitations as ionosondes – land, what makes problematic the detection of marine earthquakes
* GIM global maps could be alternative but they have sparse spatial and temporal resolution, and strongly depend on the GPS receivers density on the given territory
* New, more sophisticated techniques should be developed for the reliable detection of ionospheric precursors on the strong ionospheric variability background
* Topside sounding maybe good addition for the ocean gap filling and providing the additional ionospheric parameters

NASA Tests GPS Monitoring System for Big U.S. Quakes

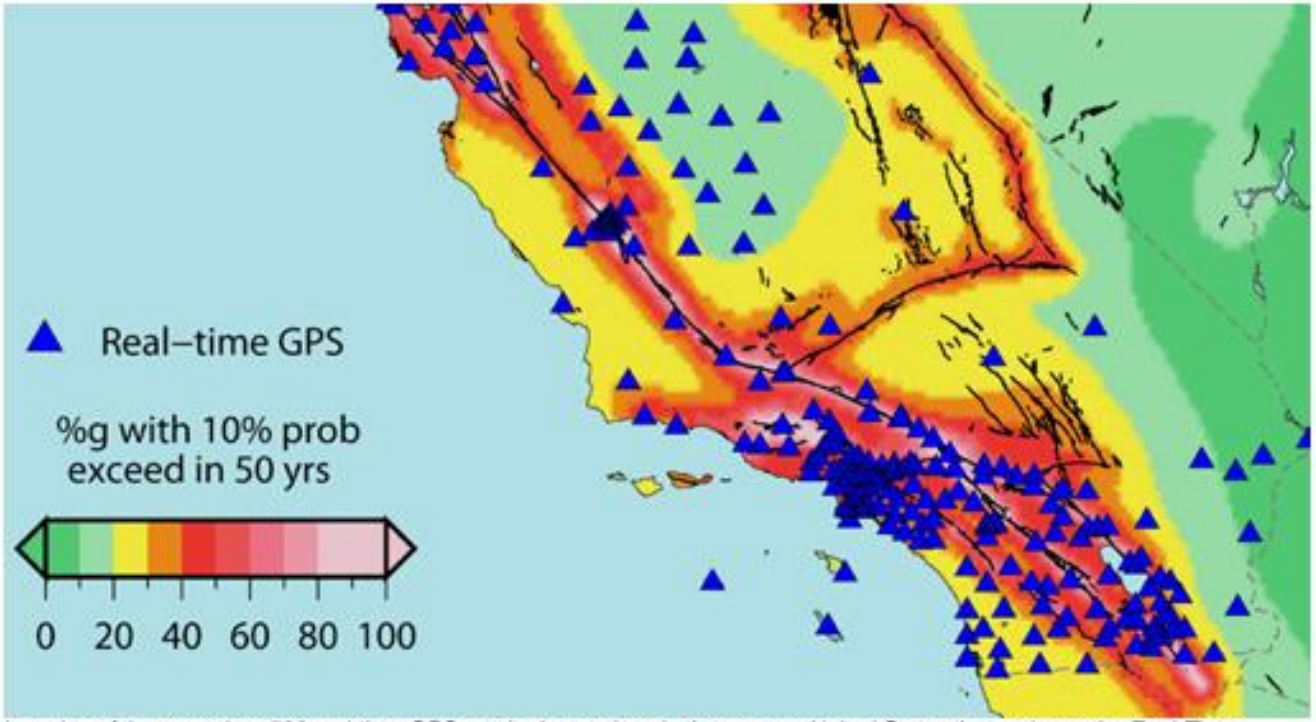

Location of the more than 500 real-time GPS monitoring stations in the western United States that make up the Real-Time Earthquake Analysis for Disaster Mitigation Network. Image credit: USGS/UC Berkeley/Scripps Institution of Oceanography
› Full image and caption

search articles submit

Most Popular

Fireball Over California/Nevada: How Big Was It?
Dawn Reveals Secrets of Giant Asteroid Vesta
12-Mile-High Martian Dust Devil Caught In Act
NASA's Spitzer Finds Galaxy With Split Personality
NASA Tests GPS Monitoring System for Big U.S. Quakes
Lecture Brings Galileo's Travels into Final Focus

You Might Like

Historic Deep Space Network Antenna Starts Major Surgery
› Read more

NASA Goes Inside a

Thank you

GEOMAGNETISM AND AERONOMY, English Translation, VOL. 35, NO. 4, FEBRUARY 1996
Russian Edition: JULY–AUGUST 1995

Wavelike structure of longitudinal variations of the nighttime equatorial anomaly

G. F. Deminova

Institute of the Terrestrial Magnetism, Ionosphere and Radio Wave Propagation

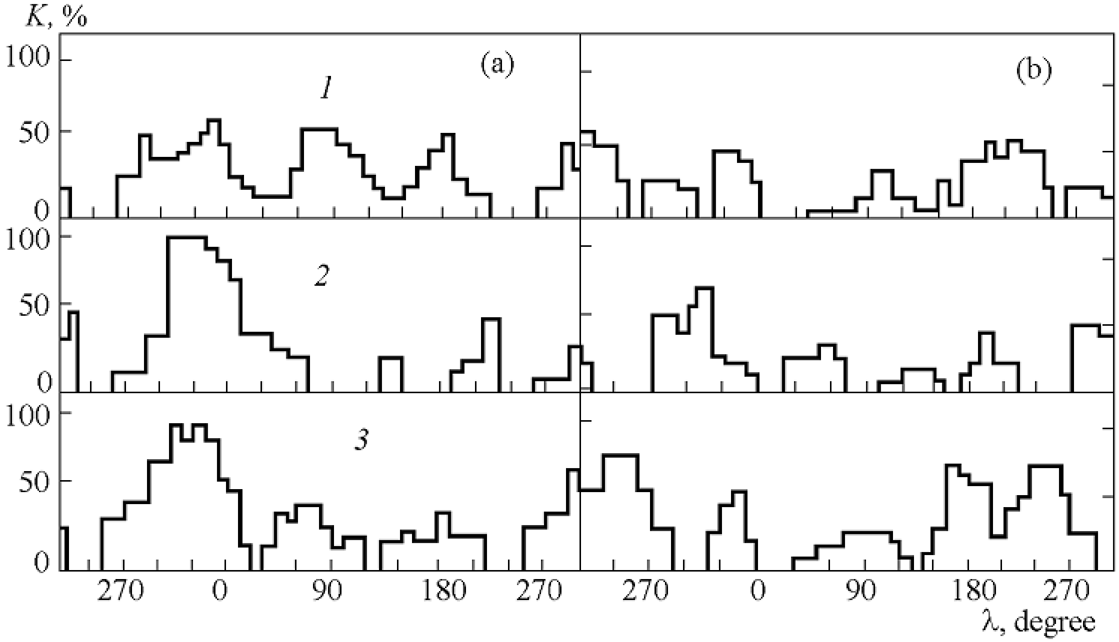

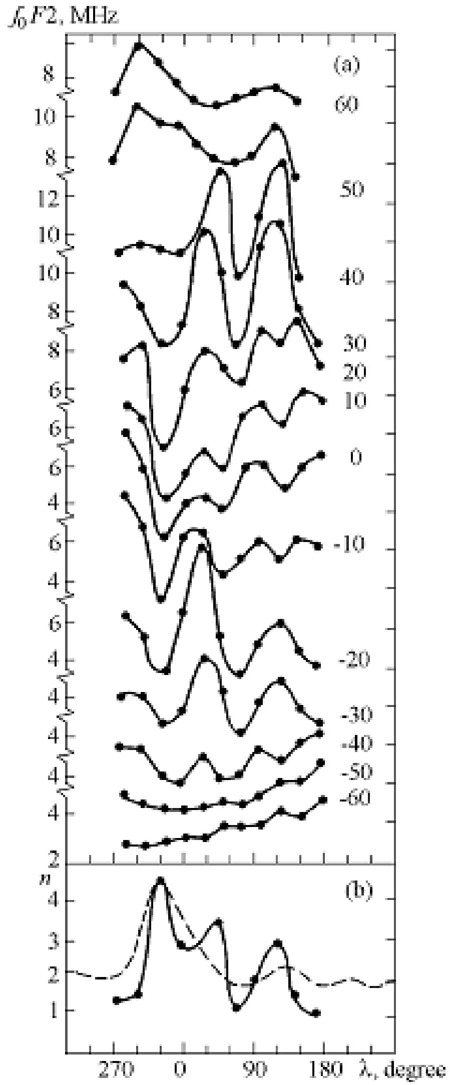

IRI Task Force Activity 2002
ICTP, Trieste

Equatorial anomaly variability as a function of the local time and the longitude

S.A.Pulinets,
Instituto de Geofísica, UNAM, México
M. Hernandez-Pajares,
Univ. Politecnica de Catalunya, Barselona, Spain
V.H.Depuev,
IZMIRAN, Russia

Equatorial anomaly global distribution for July 1979, 14:30 LT by Intercosmos-19 topside sounding data

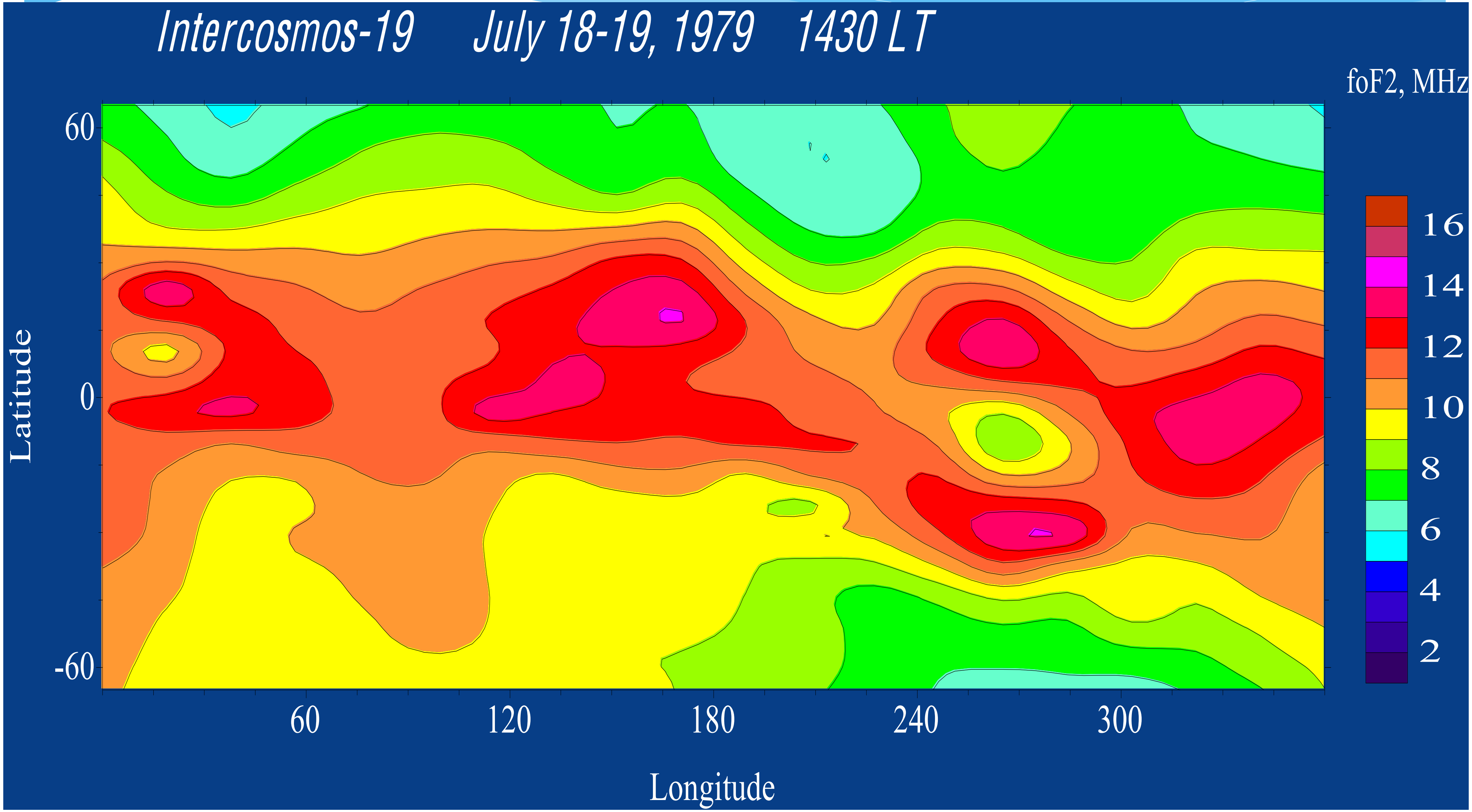

Peak and model parameters global distribution

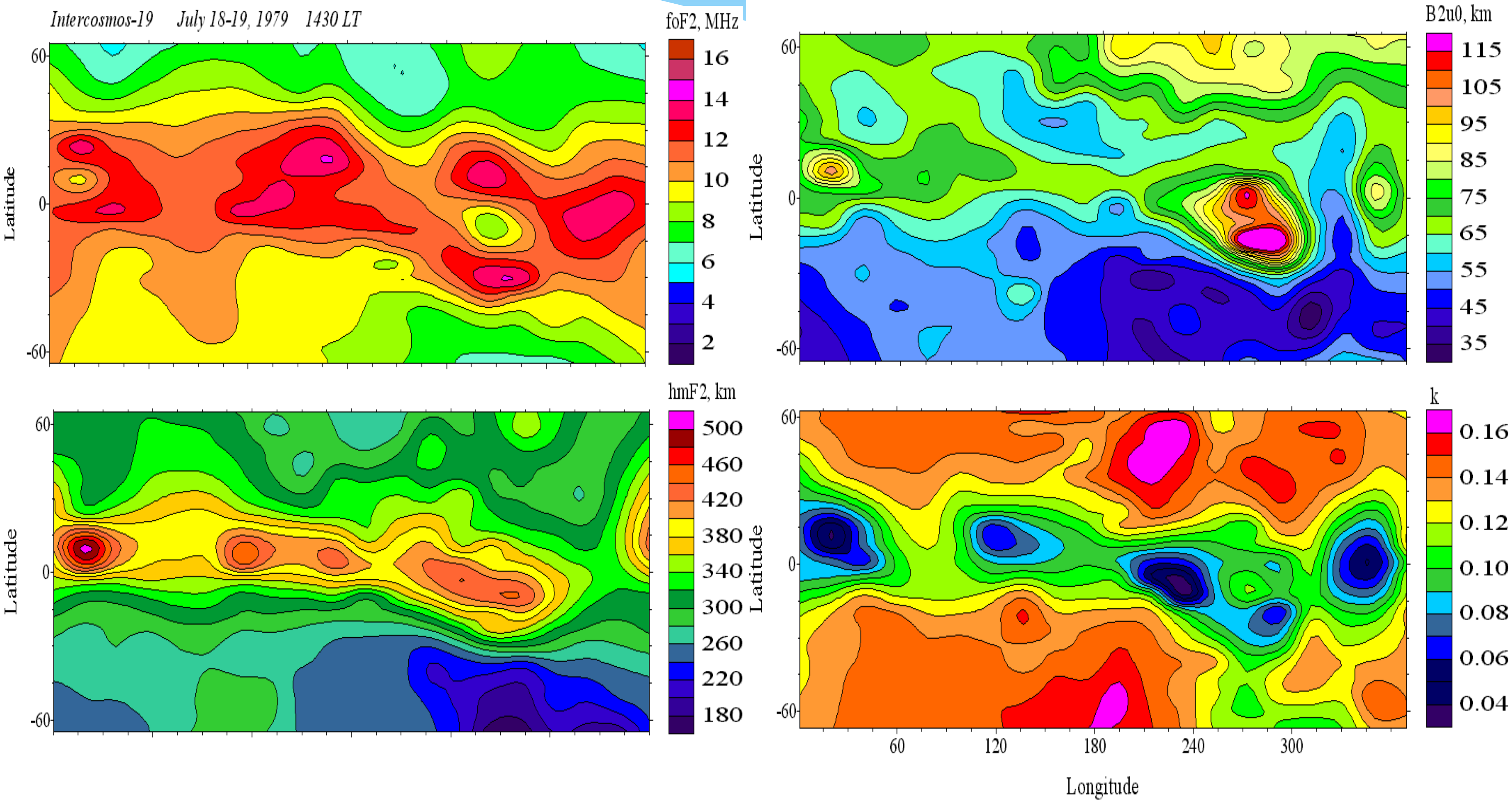

Comments on the paper of J. Love et al.

On the Reported Ionospheric Precursor of the 1999 Hector Mine, California Earthquake

Prof. Sergey Pulinets
Institute of Applied Geophysics
Moscow
pulse1549@gmail.com

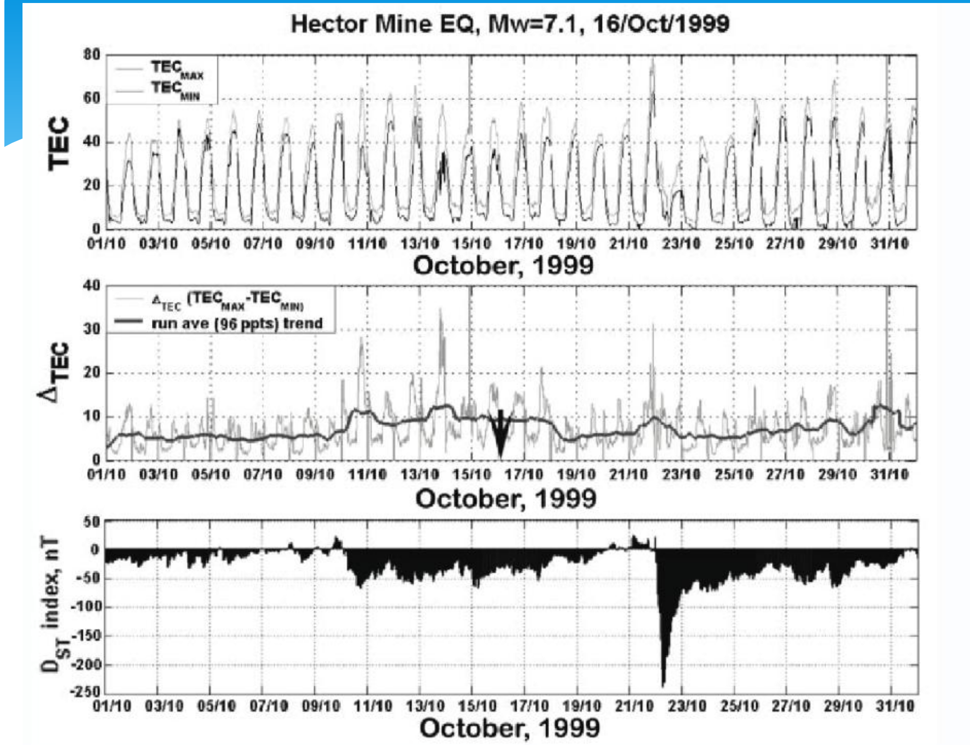

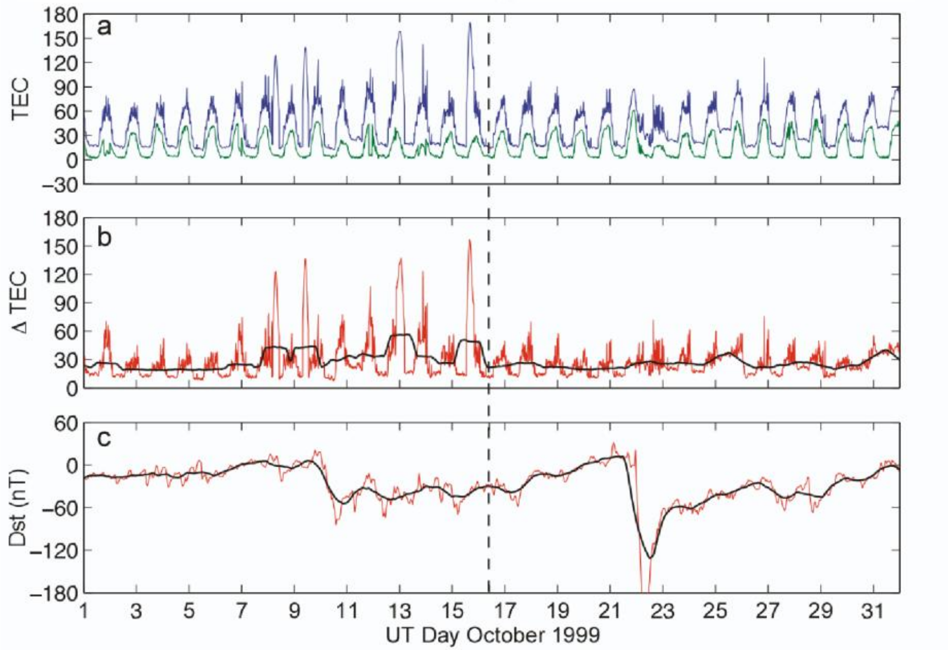

The paper of J. Love et al. is and attempt to re-analyze the GPS TEC data for period around the Hector Mine earthquake and to prove that results presented in the paper S. A. Pulinets, A. N. ...enko, L. Ciraolo, I. A. Pulinets, Special case of ... variability associated with...

Very good correspondence, even their index looks better.

Questions:

1. Why authors average the Dst index? It is absolutely incorrect because the strength of geomagnetic storm (and corresponding ionosphere reaction) are determined by the maximum value of Dst which for this storm was -237 nTl – very strong storm (by averaging authors obtained -120 – two times less)

2. Top panel of the bottom figure (blue line) if it is really TEC as it is written is absolutely incorrect. TEC **SHOULD** show reaction on geomagnetic storm on 22 October.

Here is demonstration how should look the TEC as a results of geomagnetic disturbance. Red line – vertical TEC calculated for the station *cosa1*, blue line – monthly median. Bottom panel – Dst index for October 1999. One can see one-to-one correspondence of the positive TEC deviations to the geomagnetic disturbances.

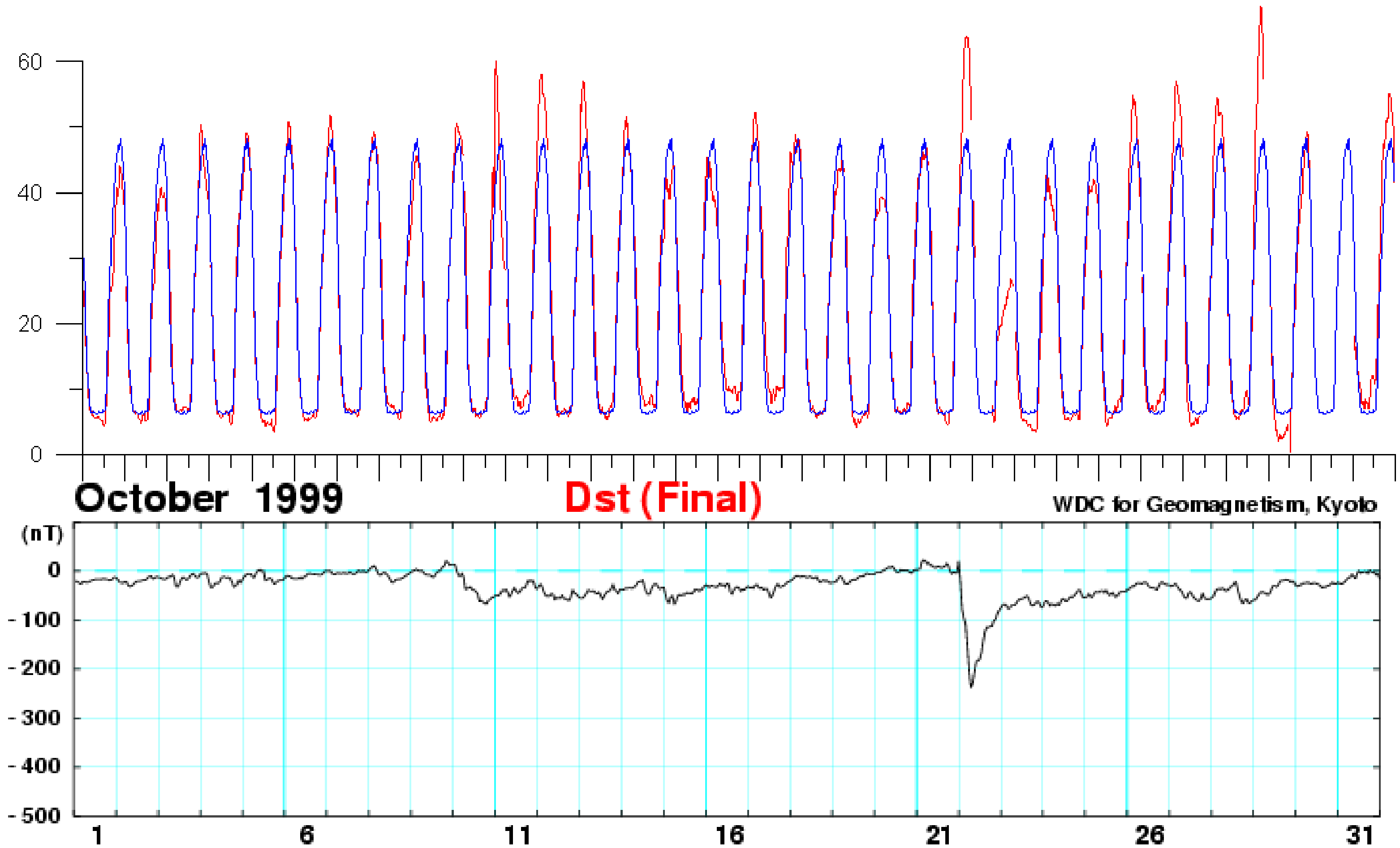

Variability index does not react on geomagnetic storms

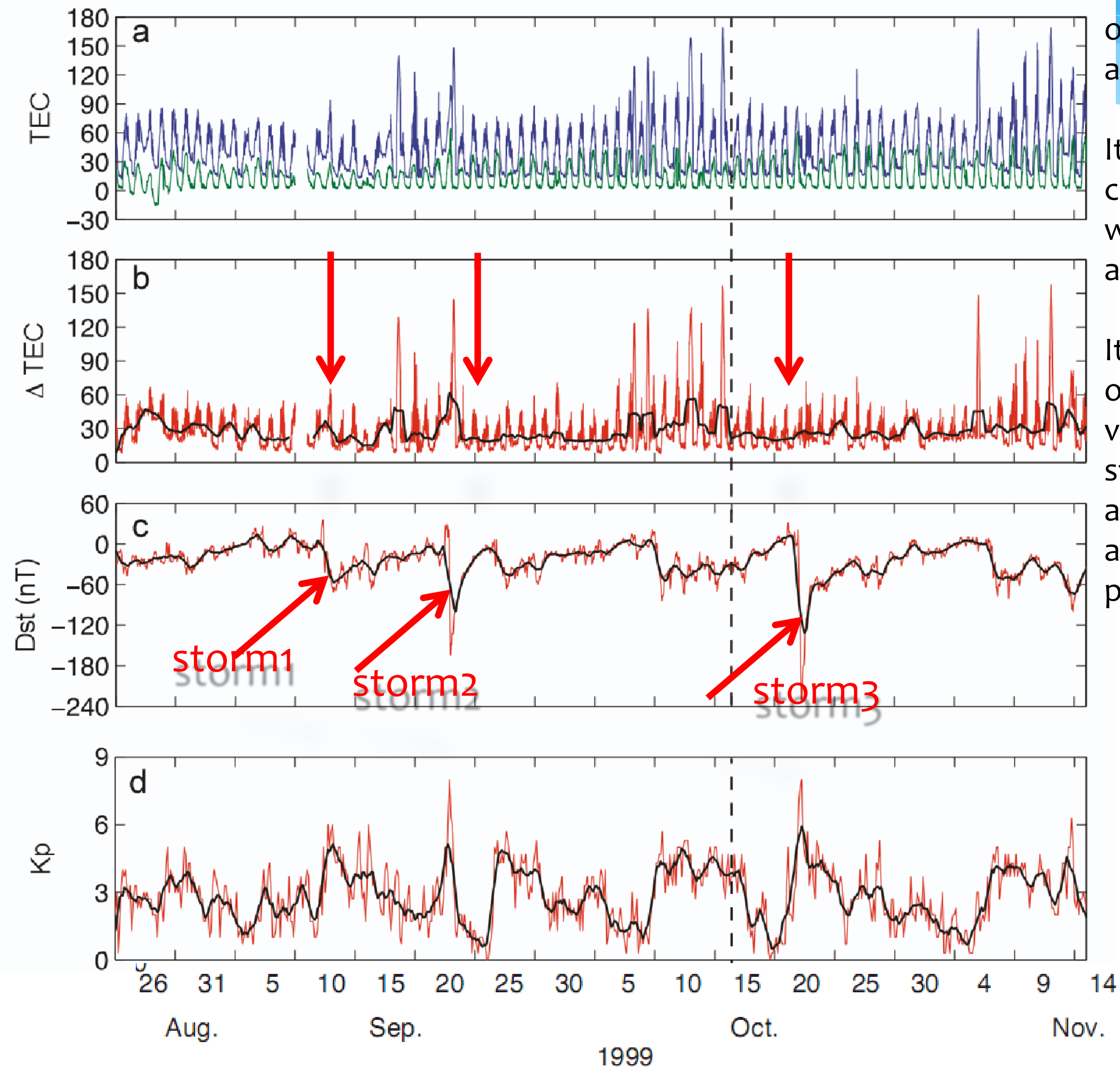

The authors extend time interval to 4 months and claim that other periods of increased variab. index indicate that it coincides with increase of Kp index and other indices of solar and geomagnetic activity.

It would be interesting to see at least one calculation of any correlation coefficient with any of indices. Otherwise it is simple allegation.

It is obvious that the strongest reaction of ionosphere and correspondent variability should coincide with the strongest geomagnetic storms. Red arrows show geomagnetic storms start and we do not see reaction both at upper panel (blue) and lower panel (red)

Storm 1 no reaction
Storm 2 ionospheric disturbance BEFORE the storm starts
Storm 3 – strongest storm for the whole period of 4 months – no reaction

So where authors see correspondence to geomagnetic actitvity?

The regional variability index was created especially to diminish effects of geomagnetic activity onto ionosphere and to underline the variability connected with the earthquake preparation. It is based on the fact that geomagnetic activity has global character while the seismo-ionospheric variability - the local character. It means that ionospheric variations stimulated by geomagnetic activity will be similar at all stations while seismo-ionospheric variability will be stronger at stations closest to the position of impending epicenter. That's why the spread in data for set of stations situated at different distances from epicenter will be larger than during geomagnetic disturbance. The most bright example – variability index before Mega-Sumatra earthquake on 26 Dec 2004. No reaction on geomagnetic storm – strongest in the year and increase before EQ.

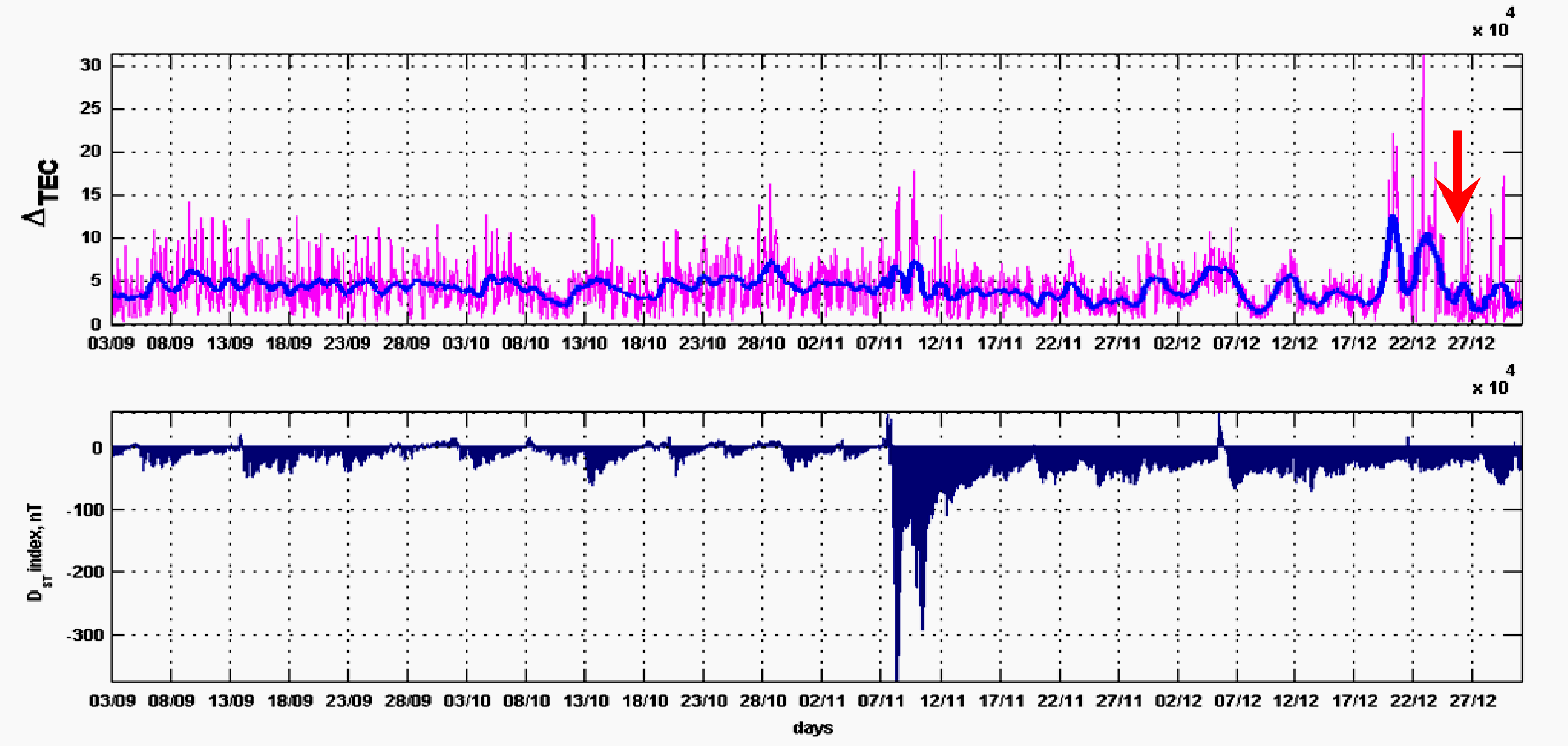

PDE	1999	09 26 161538	37.38	-117.10	9	4.5	MLBRK	... .	318
PDE	1999	09 26 201122	37.37	-117.09	9	4.4	MLBRK	... .	316
PDE	1999	10 16 094644.13	34.59	-116.27	0	7.1	MwHRV	......	0
PDE	1999	11 14 142009.41	34.84	-116.40	6	4.5	MLPAS	.F.	29

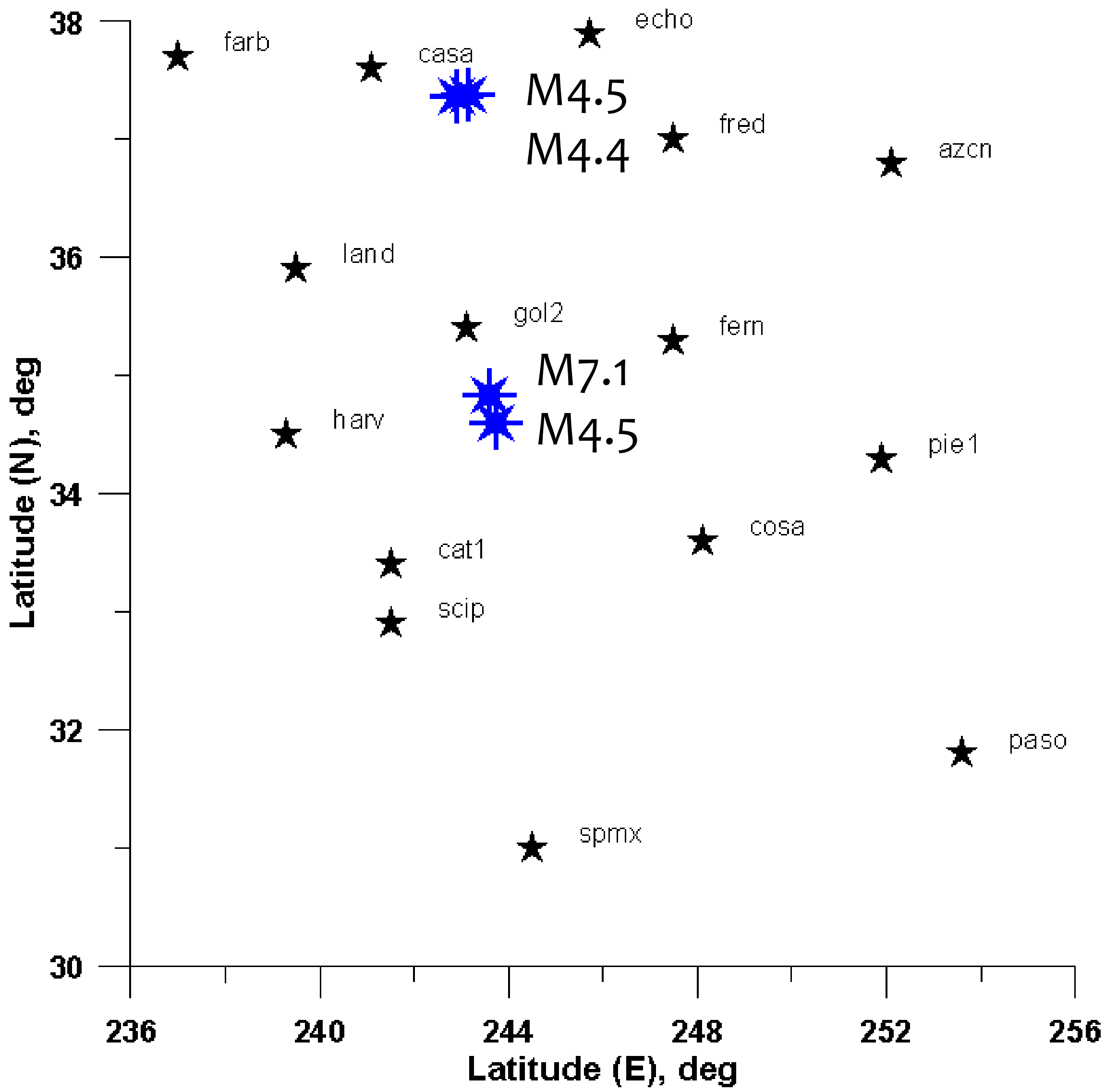

We analyzed the situation to find what could create increase of variability index within the extended time interval. Usually it considered the threshold of ionosphere sensitivity to the seismic events with M>5. But for such magnitude we see the clear area of disturbed variability. The small-scale variability (if we have station close to epicenter could be detected for lower levels. From the USGS catalog we selected double M4.4-4.5 event on 26 of September, main event on 16 October and M4.5 event on 14 November, and result is presented in the next slide.

One can clearly see that observed variability perfectly fits to our theory.